ChemPubSoc Europe

DOI: 10.1002/ejic.201600540

EurJIC European Journal of Inorganic Chemistry

Full Paper

Copper-Catalyzed Oxidation

Dual Role of Acetate in Copper(II) Acetate Catalyzed Dehydrogenation of Chelating Aromatic Secondary Amines: A Kinetic Case Study of Copper-Catalyzed Oxidation Reactions

Kesavapillai Sreenath,[a] Zhao Yuan,[a] Miguel Macias-Contreras,[a] Vasanth Ramachandran,[a] Ronald J. Clark,[a] and Lei Zhu*[a]

Abstract: Copper(II) acetate is a frequent empirical choice of the copper source in copper(II)-mediated redox reactions. The effect of the acetate counterion appears crucial but has not been adequately investigated. Herein, we report that copper(II) acetate catalyzes the aerobic dehydrogenation of chelating aromatic secondary amines. The chemoselectivity of acetate and chelating amines in this reaction provides a unique opportunity for a mechanistic study. The progression of this homogeneous reaction is monitored by using electron paramagnetic resonance spectroscopy, UV/Vis absorption spectroscopy, and manometry. The kinetic dependence on the amine substrate, copper(II), and acetate counterion, together with the results of kinetic isotope and substituent effect experiments, suggests that acetate acts both as a bridging ligand of a dinuclear catalytic center for mediating two-electron transfer steps and as a base in the turnover-limiting C–H bond-cleavage step. Upon including 1,8-diazabicyclo[5.4.0]undec-7-ene (DBU) as a surrogate base, DBU and acetate act in a complementary manner to enable a rapid, catalytic dehydrogenation reaction of a chelating secondary amine substrate. Finally, the contrasting reactivities between copper(II) acetate (promoting two-electron transfer) and copper(II) perchlorate (promoting single-electron transfer) underscores how a counterion could completely alter the mechanistic pathway of a copper-mediated oxidation reaction.

Introduction

The prevalence of +1 and +2 oxidation states of copper ensures that copper salts are effective single-electron transfer mediators in radical-involved organic transformations.[1] The majority of organic redox elementary reactions, on the other hand, entail two-electron transfer processes, of which palladium, an excellent two-electron transfer mediator but a much less-abundant element than copper, has been a major source of catalyst development.[2] The two-electron shuttling between the +1 and +3 oxidation states of a mononuclear copper center is implicated in a growing number of copper-involved reactions,[3] notably in Gilman chemistry,[3b,4] Ullmann cross-coupling,[5] and C–H functionalization reactions.[6] The ability of mononuclear copper to engage in both single- and two-electron transfer reactions was recently described by Stahl, Ribas, and co-workers.[5b,7] However, mononuclear copper(III) species have only been observed in a handful cases in which a stabilizing macrocyclic ligand[6a,6b,8] was often present,[3c,9] which casts doubt on its generality in the rapidly growing number of reported copper-mediated redox reactions.

Dinuclear copper centers are capable of mediating two-electron transfer processes through collective redox switching between the +1 and +2 oxidation states. A dicopper center may lower the activation barrier of two-electron transfer steps, similar to the cases demonstrated in dipalladium[10] and digold chemistry,[11] which would circumvent the relatively unstable mononuclear copper(III) intermediates. The utility of di- or multinuclear copper clusters in catalytic aerobic oxidation has been recognized by the inorganic and bioinorganic communities.[12] As a result, elaborated ligand-supported multinuclear complexes have been created to mimic the functions of copper-dependent oxidases and oxygenases.[13] However, the potential of dinuclear (or multinuclear) copper redox catalysis has not yet been fully materialized in synthetic chemistry development. Furthermore, copper-catalyzed oxidation methods have been developed at a rapid rate;[1b,1c,14] yet, the mechanistic clarifications of these reactions are disproportionally lagging behind.

In our investigation on the mechanism of copper(II) acetate mediated azide–alkyne cycloaddition (CuAAC) reactions,[15] we offered evidence and arguments that the copper(II) acetate dimer $[Cu_2(OAc)_4(H_2O)_2]$ mediates the inducting alkyne oxidative homocoupling (OHC)[16] stoichiometrically and the subsequent CuAAC reaction catalytically. The currently accepted mechanistic models of both OHC[16,17] and CuAAC[15,18] include copper-catalyzed two-electron transfer steps. Copper(II) acetate equilibrates in solution between monomeric and dimeric forms, depending on the solvent and additional ligand structures.[19] Given the frequent empirical choice of copper(II) acetate in copper-mediated oxidation reactions,[1c,7a,14,16,20] it is likely that the acetate-bridged dinuclear copper(II) core acts as a two-electron

[a] Department of Chemistry and Biochemistry, Florida State University, 95 Chieftan Way, Tallahassee, FL 32306-4390, USA
E-mail: lzhu@chem.fsu.edu
http://chem.fsu.edu/zhu

Supporting information for this article is available on the WWW under http://dx.doi.org/10.1002/ejic.201600540.

© 2016 Wiley-VCH Verlag GmbH & Co. KGaA, Weinheim

transfer mediator in many cases.[21] Herein, we report our first case study, which is the copper-dependent dehydrogenation of chelating secondary amines, in testing this hypothesis.[22–24]

Results and Discussion

Reactivity Profile

Secondary amine **1** (Scheme 1) was dehydrogenated rapidly to **1**-im upon treatment with 1 mol-equiv. of $Cu(OAc)_2{\cdot}H_2O$ in CH_3CN (Table 1, Entry 1) under aerobic conditions (i.e., open to air). A minor product of a deep-red color was also observed (absorption centering at 505 nm, see Figure 1a), which upon demetalation was characterized as the regiospecifically hydroxylated derivative of **1**-im (i.e., **1**-im-OH) (see Figures S1–S4 in the Supporting Information for characterization data). Titration of $Cu(OAc)_2{\cdot}H_2O$ into a CH_3CN solution of **1**-im-OH reconstituted the absorption band of the reddish species (Figure 1b), to which the formula [Cu(**1**-im-O)(OAc)] was tentatively assigned. The reaction shown in Scheme 1 may represent a simple model of both copper-dependent oxidase (**1** to **1**-im) and oxygenase (**1**-im to **1**-im-OH) activities,[7a,25] which entail benzylic-like C(sp^3)–H and aromatic C(sp^2)–H functionalizations, respectively. In this article, the investigation of the mechanism of the transformation from **1** into **1**-im is described, whereas that on the formation of **1**-im-OH is deferred to a later study.

Nonchelating compounds **2** and **3** (Table 1, Entries 2 and 3) did not undergo dehydrogenation under the same conditions. Replacing $Cu(OAc)_2{\cdot}H_2O$ with $Cu(ClO_4)_2{\cdot}6H_2O$ (Table 1, Entry 4), which is a stronger single-electron oxidant,[26] resulted in a much lower conversion of **1** to a mixture of undefined products [other tested copper(II) salts were also not as effective as $Cu(OAc)_2{\cdot}H_2O$; see Table S1]. If the reaction mixture was maintained under anaerobic conditions (Table 1, Entry 5), the reaction proceeded at a reduced rate.[27] Aliphatic secondary amines (Table 1, Entries 6 and 7) and a tertiary amine (**1**-Me in Table 1, Entry 8) did not react. Upon installing an electron-withdrawing group at the *para* position of the anilinyl moiety, the reaction slowed down (Table 1, Entries 9–13). Finally, *gem*-dimethyl substrate **11** did not undergo dehydrogenation, which was expected, or hydroxylation (Table 1, Entry 14). These observations are summarized as follows: (1) the substrate needs to be a chelating aromatic secondary amine; (2) molecular oxygen is not required, but it accelerates the reaction; (3) $Cu(OAc)_2{\cdot}H_2O$ is by far the most effective copper(II) salt; (4) oxidation of the anilinyl moiety appears to be a kinetically significant step; (5) a substrate that is unable to dehydrogenate (e.g., *gem*-dimethyl-containing **11**) cannot be hydroxylated.

Electron Paramagnetic Resonance Spectroscopy

Different techniques were applied to monitor the changes in the key components over the course of this homogeneous reac-

Table 1. Reactivity profile of copper(II) acetate mediated dehydrogenation.[a]

Entry	Substrate	Conversion	Time	Anion	Air
1	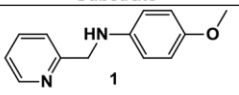 **1**	> 95%	5 min	AcO^-	Y
2	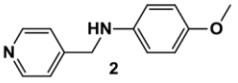 **2**	0	24 h	AcO^-	Y
3	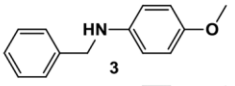 **3**	0	1 h	AcO^-	Y
4	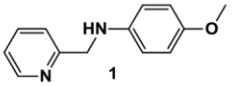 **1**	< 11%[b]	5 min	ClO_4^-	Y
5	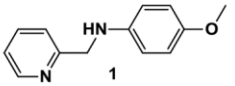 **1**	17%[c]	5 min	AcO^-	N
6	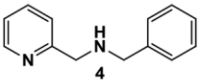 **4**	0	24 h	AcO^-	Y
7	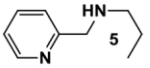 **5**	0	24	AcO^-	Y
8	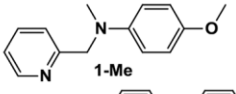 **1-Me**	0	24 h	AcO^-	Y
9	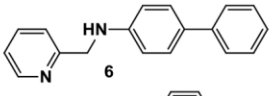 **6**	> 95%	5 min	AcO^-	Y
10	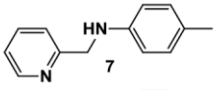 **7**	> 95%	30 min	AcO^-	Y
11	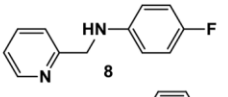 **8**	> 95%	1 h	AcO^-	Y
12	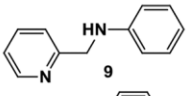 **9**	> 95%	2 h	AcO^-	Y
13	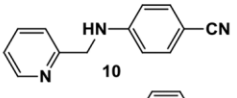 **10**	0	24 h	AcO^-	Y
14	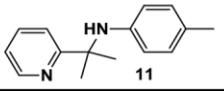 **11**	0	24 h	AcO^-	Y

[a] Procedure: An amine (0.08 mmol) substrate was dissolved in CH_3CN (4.0 mL) in a round-bottom flask equipped with a magnetic stir bar. $Cu(OAc)_2{\cdot}H_2O$ (0.08 mmol) was added, and the mixture was stirred at r.t. for the listed time. An ethylenediaminetetraacetic acid (EDTA) solution (5 mL, 0.1 M, pH > 10) was added, and the mixture was extracted with CH_2Cl_2 (2 × 5.0 mL). The organic layer was separated and dried with anhydrous Na_2SO_4 or K_2CO_3. The solvent was removed under reduced pressure to obtain the crude product, which was analyzed by ^1H NMR spectroscopy (500 MHz, $CDCl_3$). [b] A complicated mixture of several compounds was observed. The consumption of compound **1** was at best 11 %. [c] If the amount of $Cu(OAc)_2{\cdot}H_2O$ was doubled to 0.16 mmol so that $Cu(OAc)_2{\cdot}H_2O$ was presumed to be the stoichiometric oxidant, the conversion went up to 26 % in 5 min.

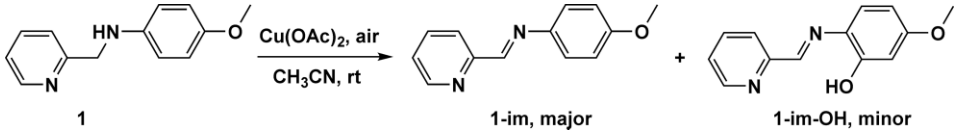

Scheme 1. $Cu(OAc)_2$-mediated oxidation of secondary amine **1**.

© 2016 Wiley-VCH Verlag GmbH & Co. KGaA, Weinheim

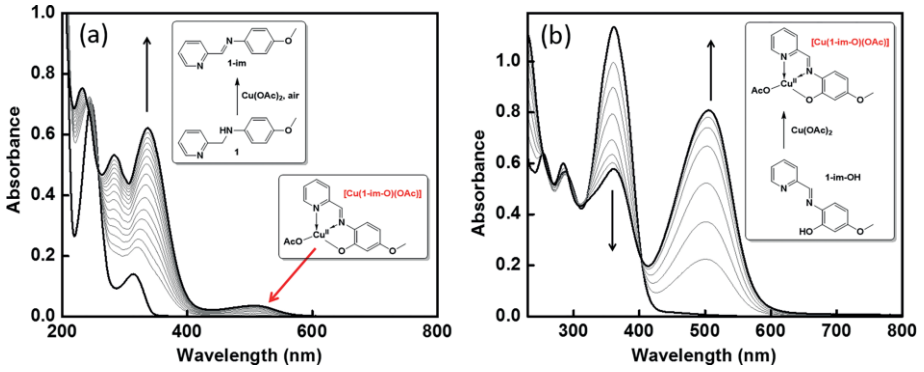

Figure 1. (a) Progression of the aerobic oxidation of **1** (0.06 mM) in the presence of $Cu(OAc)_2 \cdot H_2O$ (0.05 mM) in CH_3CN. The absorption of the reddish copper(II) complex [Cu(**1**-im-O)(OAc)] is indicated by a red arrow. (b) Absorption spectral change of **1**-im-OH (0.1 mM) in CH_3CN upon addition of $Cu(OAc)_2 \cdot H_2O$ (0–0.1 mM).

tion. The change in the copper oxidation state and/or nuclearity was monitored by electron paramagnetic resonance (EPR) spectroscopy. The EPR signal of the copper(II) acetate dimer $[Cu_2(OAc)_4(H_2O)_2]$ in CH_3CN was undetectable at room temperature (Figure S6). The addition of pyridine led to a small enhancement in the intensity of the EPR signals (Figure 2a). The addition of nonchelating (e.g., compound **2**, Figure S7) or weakly chelating (e.g., compound **10**, Figure 2b) amines also barely affected the spectrum of copper(II) acetate. However, mixing of copper(II) acetate with chelating amines, either secondary (e.g., compounds **1**, **4**, and **8**) or tertiary (e.g., compound **1**-Me, Figure 2d), aromatic or otherwise, led to the immediate appearance of a four-line signal characteristic of mononuclear isotropic hyperfine splitting ($g_{isotropic}$ = 2.1298; $A_{isotropic}$ = 67 Gauss).[28] Under aerobic conditions, the intensity of the EPR spectra involving reactive substrates decreased over time (e.g., compound **1** in Figure 2c), whereas that of nonreacting substrates underwent little change (e.g., compound **4** in Figure S8 and **1**-Me in Figure 2d). Secondary chelating amines with electron-poor anilinyl groups, such as cyano-substituted **10**, hardly amplified the EPR signal of $Cu(OAc)_2 \cdot H_2O$ (Figure 2b). Therefore, their lack of reactivity of **10** was attributed to poor binding with copper(II).

The process depicted in Scheme 2 accounts for the EPR data of copper(II) acetate upon binding with various substrates or ligands. The lack of EPR signals for copper(II) acetate and its pyridine complex is attributed to antiferromagnetic coupling between the two copper(II) centers in the acetate-bridged dimers,[29] which appears to dominate in CH_3CN. Upon interacting with a pyridyl-containing secondary or tertiary amine, the

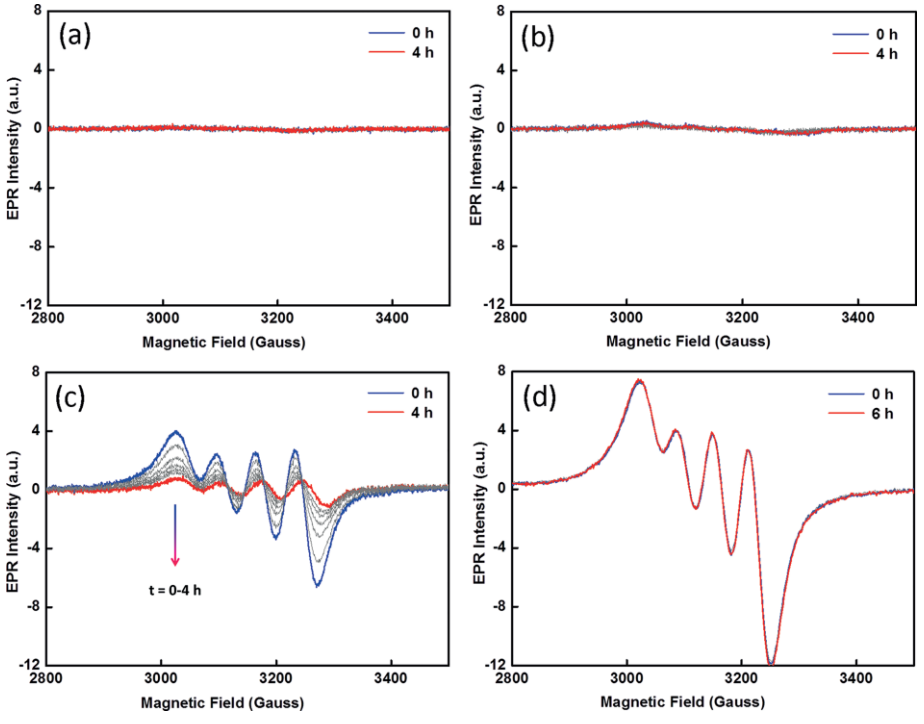

Figure 2. The EPR (X-band) spectra of $Cu(OAc)_2 \cdot H_2O$ (10 mM in CH_3CN) in the presence of (a) 10 mM pyridine, (b) 10 mM of **10**, (c) 10 mM of **1**, and (d) 10 mM of **1**-Me over the allotted time. The *y* axes show the EPR intensity in arbitrary units of the same scale.

© 2016 Wiley-VCH Verlag GmbH & Co. KGaA, Weinheim

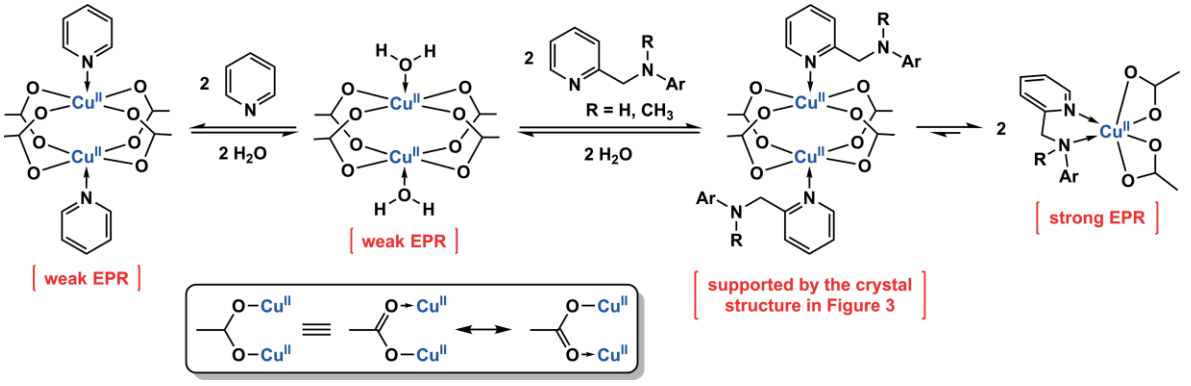

Scheme 2. Amine substrate binding with copper(II) acetate in acetonitrile. Acetate–copper(II) bonding is simplified as shown in the box, that is, a Cu–O bond in the scheme counts for a half bond.

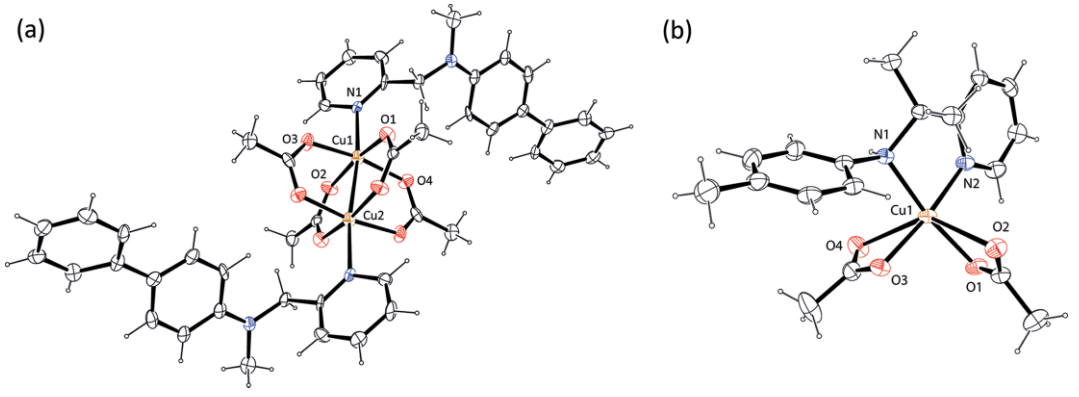

Figure 3. ORTEP views (50 % probability ellipsoids) of (a) the asymmetric unit of $[Cu_2(\mathbf{6}\text{-Me})_2(OAc)_4]$; selected distances [Å]: Cu1–N1 2.219(5), Cu1–Cu2 2.644(1), Cu1–O1 1.954(5), Cu1–O2 1.948(5), Cu1–O3 1.974(5), Cu1–O4 1.975(5); and (b) $[Cu(\mathbf{11})(OAc)_2]$; selected distances [Å]: Cu1–N1 1.985(2), Cu1–N2 2.035(2), Cu1–O1 1.958(2), Cu1–O2 2.597(2), Cu1–O3 1.957(2), Cu1–O4 2.572(2).

axial water ligands are replaced by the pyridyl portion of the amine, as suggested by the dimeric structure of $[Cu_2(\mathbf{6}\text{-Me})_2(OAc)_4]$ (Figure 3a). The dimer equilibrates with the EPR-positive monomers, in which the chelating amine ligand is bidentate as suggested by the structure of $[Cu(\mathbf{11})(OAc)_2]$ (Figure 3b).

Following the binding of a secondary chelating amine substrate with copper(II) acetate, which increased the abundance of the monomeric copper(II) complex and consequently produced a strong EPR signal, the decrease in the EPR intensity accompanied the progress of the dehydrogenation reaction (such as **1** in Figure 2c). A couple of scenarios may account for the drop in EPR intensity as the reaction proceeds: (1) the copper oxidation state changes from the paramagnetic +2 to the EPR silent +1 state; (2) an antiferromagnetically coupled copper(II) dimer is reconstituted owing to the fact that the binding of the imine product to copper(II) is weaker than that of the amine reactant. The EPR signal of secondary amine **8** (Figure 4a) prepared under anaerobic conditions also decreased as the reaction progressed, which supported the former scenario that copper(II) was reduced to copper(I). The reddish color appeared at the top of the EPR tube as a result of the slow entry of air through the sealing grease and diffused down overtime, which suggested that the formation of the reddish copper(II)/**8**-im-OH complex was O_2-dependent.

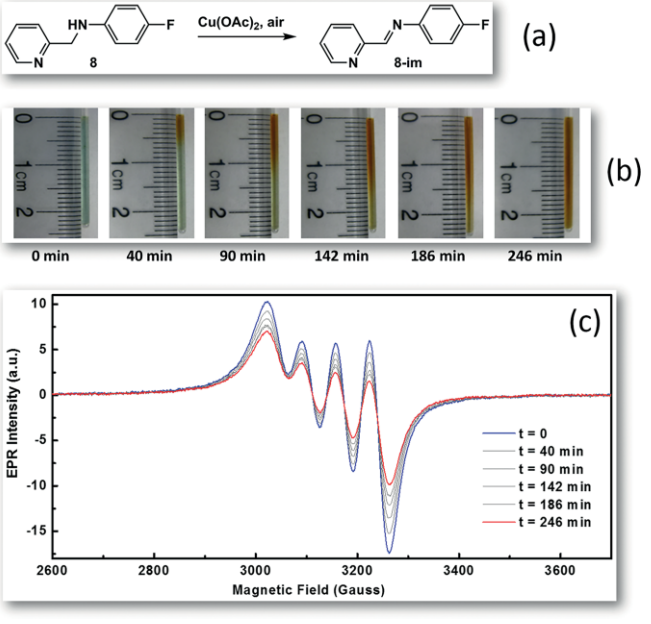

Figure 4. (a) Conversion of amine **8** into imine **8**-im; (b) photographs of the EPR tube containing **8** (10 mM) and $Cu(OAc)_2{\cdot}H_2O$ (10 mM) in CH_3CN, which was sealed with grease, overtime undisturbed; (c) the corresponding EPR spectra at the time intervals shown in panel b.

© 2016 Wiley-VCH Verlag GmbH & Co. KGaA, Weinheim

Manometry

O_2 accelerates the dehydrogenation reaction, as concluded by comparing the data from Entries 1 and 5 of Table 1. The O_2 consumptions with a few amine substrates were monitored by manometry.[6c,30] The pressure change from 1 atm of air in a closed reaction vessel was recorded for various secondary and tertiary amines (Figure 5). Only chelating aromatic secondary amines with adequate electron density on the anilinyl moiety afforded a substantial reduction in pressure (e.g., compounds **1** and **8** in Figure 5). Neither tertiary amine **1**-Me, which binds copper(II) strongly as shown by EPR spectroscopy (Figure 2d), nor *p*-cyano-substituted secondary amine **10**, which at best weakly associates with copper(II) (Figure 2b), enabled O_2 uptake. Therefore, the consumption of O_2 was concurrent with the progress of the dehydrogenation reaction under aerobic conditions. The molar ratio between O_2 and the amine reactant was ca. 1:2 (Figure S9, Table S2), which suggested that O_2 was reduced to H_2O.

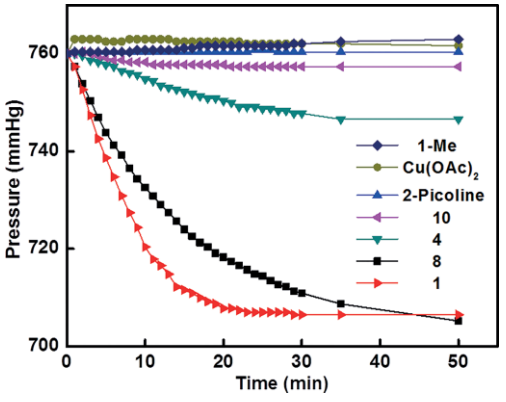

Figure 5. Pressure of the reaction vessel (total volume = 35 mL) over time of mixtures of amines (**1**, **1**-Me, **4**, **8**, **10**, and 2-picoline, 0.25 M in CH_3CN) and $Cu(OAc)_2{\cdot}H_2O$ (0.25 M).

Linear Free-Energy Relationship and Kinetic Isotope Effect

The imine production was monitored by using UV/Vis absorption spectroscopy (e.g., Figure 1a).[32] The linear free-energy relationship (LFER) and deuterium kinetic isotope effect (KIE) were determined by using this method. If the substituent X (Scheme 3) was varied, an LFER against σ_{para}^{+} was observed (Figure 6a).[33] A ϱ value of –1.0 suggested that electron density of the anilinyl group was decreasing en route to the transition-state structure of the turnover-limiting step, or a step of kinetic relevance. This observation discounted the possibility that amine deprotonation was turnover-limiting, of which the opposite LFER was expected. Rather, a step involving anilinyl oxidation was kinetically significant. The primary KIE (k_H/k_D = 2.5, Figure 6b), determined by comparing the rates independently acquired by using protio and deuterio substrates,[34] indicated that the C–H bond-cleavage step was turnover-limiting.[35]

On the basis of the reactivity profile data in Table 1 in conjunction with the LFER and KIE observations, it is possible to determine the relative timing of the three key steps: deprotonation of the N–H and C–H bonds and oxygenation of the substrate/copper complex. The fact that tertiary amine **1**-Me is unable to react (Table 1, Entry 8) suggests that N–H deprotonation needs to occur before the turnover-limiting step. The primary KIE suggests that C–H bond cleavage is turnover-limiting. Oxygenation of the substrate before dehydrogenation was not observed. Consistent with the early-dehydrogenation model, an oxygenated secondary aromatic amine was unable to dehydrogenate if subjected under the reported reaction conditions (data not shown). Furthermore, *gem*-dimethylated compound **11** under the reaction conditions failed to afford any anilinyl hydroxylation product (Table 1, Entry 14), which further confirms that oxygenation occurs after, or simultaneously with, C–H bond cleavage.

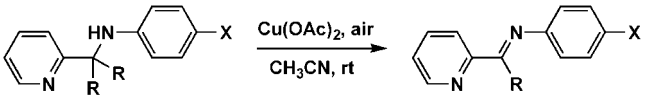

Scheme 3. Reaction for the linear free-energy relationship (LFER) and kinetic isotope effect (KIE) experiments. Substrates of the KIE study (k_H/k_D = 2.5): R = H/D, X = OCH_3; substrates of the LFER experiment (ϱ = –1.0): R = H, X = H, OCH_3, *i*Pr, CH_3, Ph, I, and F.[31]

On the basis of the analysis at this stage, the validities of the possible dehydrogenation/copper-oxygenation sequences (Scheme 4) were assessed. The chelating amine substrate acts as a bidentate ligand for copper(II). The acetate counterion acts as an internal base to deprotonate the secondary amine to afford copper(II) amido complex **I**. The internal base function of the acetate (or other carboxylate or carbonate) counterions has been proposed in $Pd(OAc)_2$-catalyzed[36] and, more recently, in $Cu(OAc)_2$-catalyzed C–H functionalization reactions.[37]

From intermediate **I**, four possible pathways are illustrated in Scheme 4. In the mononuclear two-electron transfer pathway (Scheme 4a), **I** undergoes base-promoted C–H cleavage concurrent with the two-electron reduction of the copper(II) center to produce dead-end copper(0) species **III**. The dinuclear two-electron transfer pathway (Scheme 4b) is facilitated by the bridging ability of acetate to afford dicopper(II) intermediate **IV**. Deprotonation of the C–H bond would release two electrons that are collectively taken in by the two copper(II) centers to afford dicopper(I) intermediate **V**. Transition from **IV** to **V** could be either a concerted two-electron transfer that flips the oxidation state of both copper centers from +2 to +1 or a stepwise sequence led by the disproportionation of copper(II) to copper(III) and copper(I), which is followed by 2e reduction at the copper(III) center.[6a,6c,30] O_2 quickly traps the nascent dicopper(I) center in **V** to form μ-η^1:η^1-peroxo dicopper(II) intermediate **VI**, which could be the precursor of the oxygenation agent to afford the hydroxylated minor product. On the basis of the observations of the LFER and KIE experiments, the conversion from **IV** into **V** should be turnover-limiting (TOL).

On the basis of the suggestion of a reviewer, a β-hydride elimination pathway is included as Scheme 4c. The mononuclear intermediate after β-hydride elimination (**VII**) would undergo either reductive elimination or deprotonation to **III**, the unlikely dead-end Cu^0 species. Intermediate **VII** could potentially be transformed through the assistance of another copper(II) to intermediate **V** in Scheme 4b. We did not consider

© 2016 Wiley-VCH Verlag GmbH & Co. KGaA, Weinheim

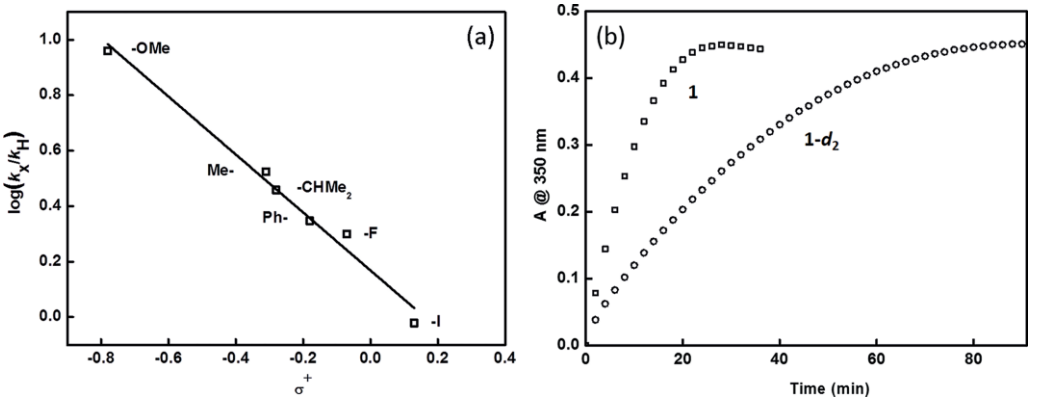

Figure 6. (a) Hammett plot for the reactions of various amines with $Cu(OAc)_2 \cdot H_2O$ in CH_3CN. (b) Absorption changes at 350 nm versus time for amines (50 μM); **1** (squares) and **1**-d_2 (circles) upon reaction with $Cu(OAc)_2 \cdot H_2O$ (50 μM) in CH_3CN.

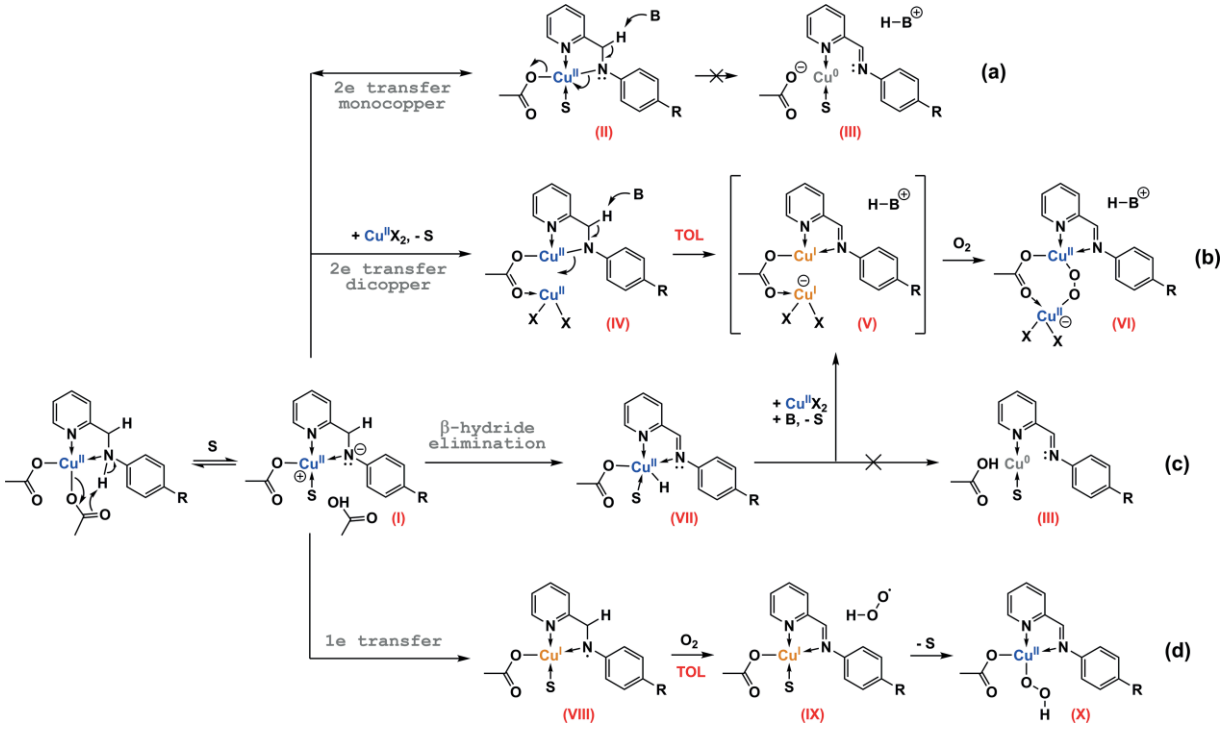

Scheme 4. Possible deprotonation/copper-oxygenation sequences. Dative bonds illustrate the lone-pair contributions from the ligands. 0, +1, and +2 oxidation states of copper are color-coded as gray, orange, and blue, respectively. TOL: turnover-limiting. S: a monodentate coordinating solvent, e.g., CH_3CN; X: a singly-charged counterion.

the β-hydride elimination pathway further owing to its lack of precedence in copper(II)-mediated oxidation reactions and its lack of base dependence, which was observed in the dehydrogenation reaction in the current work.

Lastly, single-electron transfer from the amido ligand to the copper(II) center could occur after the formation of intermediate **I** to afford **VIII** (Scheme 4d). Turnover-limiting hydrogen atom abstraction, on the basis of the KIE data, from **VIII** by O_2 results in intermediate **IX** and a hydroperoxy radical, which subsequently oxidizes the copper(I) center to form copper(II)–hydroperoxy complex **X**. The pathway shown in Scheme 4d, which involves proton transfer followed by hydrogen-atom transfer, is similar to the proposal of Maseras and co-workers on macrocyclic amine oxidation by a mononuclear copper(II) complex.[38]

The pathways shown in Scheme 4b,d were considered further, because they do not end with a Cu^0 species. They differ in (1) the kinetic order of copper(II), (2) the dependence on O_2, (3) the dependence on a base, and (4) the function of the acetate ion. A second-order dependence on copper(II) is expected for Scheme 4b, whereas Scheme 4d requires first-order kinetics in copper. Contrary to the mononuclear pathway in Scheme 4d, which requires O_2 (or another hydrogen atom abstracting free radical agent), the dinuclear pathway in Scheme 4b could proceed anaerobically if copper(II) is provided stoichiometrically. Finally, acetate acts as both a base and a bridging ligand in

© 2016 Wiley-VCH Verlag GmbH & Co. KGaA, Weinheim

Scheme 4b, whereas the route in Scheme 4d only requires a base to reach early copper(II) amido intermediate **I**, following which the acetate appears to be a spectator ion. The fact that the dehydrogenation of **1** does proceed under the anaerobic conditions (point #2), albeit at a slower rate than the open-to-air reaction, favors Scheme 4b. The experiments described in the following subsections were performed to distinguish the pathways illustrated in Scheme 4b,d by looking at the differences raised in points #1, #3, and #4.

Kinetic Orders of Reaction Components

The kinetic orders of amine **1** and $Cu(OAc)_2{\cdot}H_2O$ were determined by using the initial-rate method under the open-to-air conditions. Amine exhibited saturation kinetic behavior (Figure 7a,b), which suggests a fast binding equilibrium between **1** and the copper catalyst prior to the turnover-limiting step. The kinetic order of $Cu(OAc)_2{\cdot}H_2O$ was 1.9 (Figure 7c), consistent with a dinuclear transition-state structure for the turnover-limiting step, and a mononuclear resting state of the copper catalyst.[39] Similar scenarios have been reported in palladium(II)-catalyzed C–H functionalization reactions.[40]

To decouple the functions of copper(II) and the acetate ion, $Cu(ClO_4)_2{\cdot}6H_2O$ was used as the copper(II) source, and the reaction progress was monitored by using UV/Vis absorption spectroscopy in the presence of increasing amounts of Bu_4NOAc (Figure 8). Without Bu_4NOAc, very little absorption change was observed over 40 min (Figure 8a). The broad peak centered at 490 nm could be the absorption of the radical cation (or a derivative thereof) resulting from the single-electron oxidation of the *p*-methoxyanilinyl group by $Cu(ClO_4)_2{\cdot}6H_2O$.[41] A control experiment to test the radical cation interpretation will be described after the discussion on the data in Figure 8.

In the presence of 0.75 equiv. Bu_4NOAc relative to the amount of copper(II), the presumed radical cation band at 490 nm was diminished, yet no reaction occurred over the same time period (Figure 8b). This observation suggested that the addition of the acetate ion reduced the ability of copper(II) as a single-electron oxidant. This possibility contradicts the mechanistic proposal illustrated in Scheme 4d, in which the addition of acetate would have aided the formation of radical species **VIII**.

Upon increasing the Bu_4NOAc concentration up to 1.75 equiv. [relative to that of copper(II)], the reaction proceeded to afford both **1**-im (centering at 350 nm) as the major product and **1**-im-OH [centering at 505 nm as its copper(II) complex] as the minor component (Figure 8c). The rate was enhanced in the presence of 2.5 equiv. of Bu_4NOAc relative to the amount of copper(II) (Figure 8d).

The absorption band centering on 490 nm in Figure 8a is postulated as the radical cation of the anilinyl group from the single-electron transfer to $Cu(ClO_4)_2{\cdot}6H_2O$. On the basis of the work of Stahl and co-workers,[42] an aryl radical cation resulting from single-electron oxidation from a copper(II) center can be halogenated by a halide ion. The hypothesis of anilinyl radical cation formation was then tested by including LiCl in the reaction mixture to trap the purported radical cation. As shown in Scheme 5a, in addition to being dehydrogenated, compound **1** was also chlorinated to **1**-Cl[43] upon treatment with a combination of $Cu(ClO_4)_2{\cdot}6H_2O$ and LiCl. Tertiary amine **1**-Me, under the

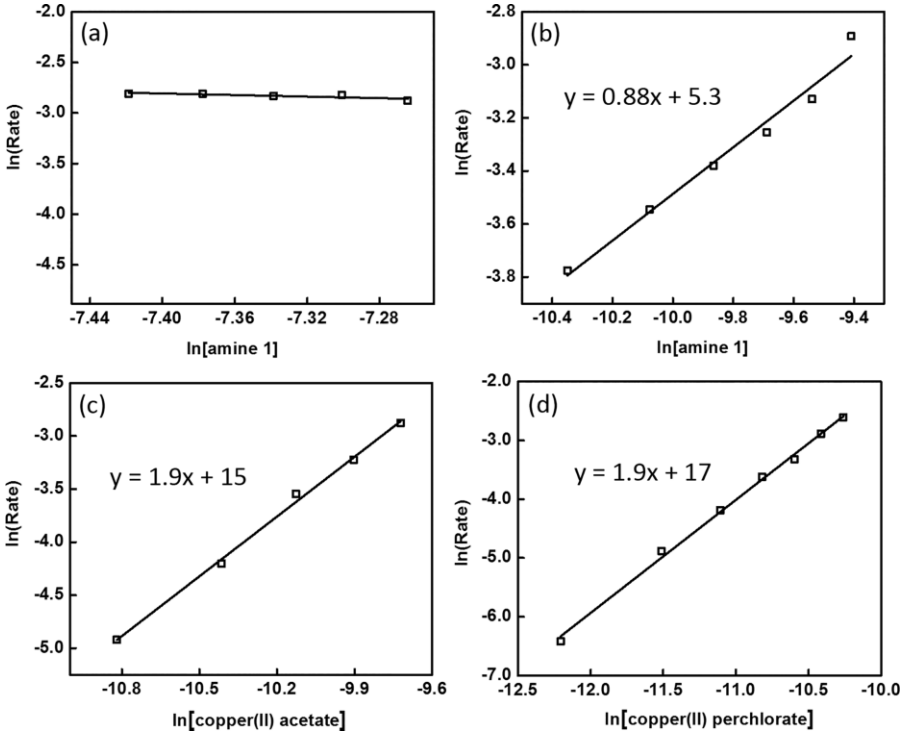

Figure 7. Log plots of the initial rate dependence on the concentrations of (a) amine **1** (600–700 μM) in the presence of $Cu(OAc)_2{\cdot}H_2O$ (50 μM), (b) amine **1** (32–82 μM) in the presence of $Cu(OAc)_2{\cdot}H_2O$ (65 μM), (c) $Cu(OAc)_2{\cdot}H_2O$ (20–60 μM) in the presence of compound **1** (0.56 mM), and (d) $Cu(ClO_4)_2{\cdot}6H_2O$ (5–35 μM) in the presence of **1** (100 μM), DBU (80 μM), and Bu_4NOAc (30 μM).

© 2016 Wiley-VCH Verlag GmbH & Co. KGaA, Weinheim

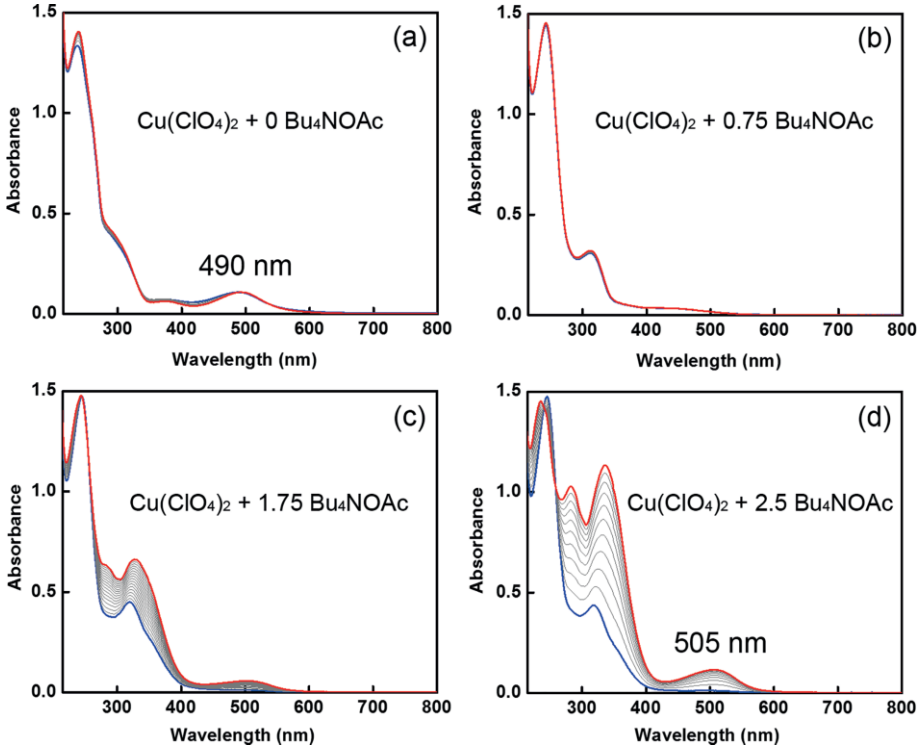

Figure 8. Absorption spectra over 40 min (2 min interval) of amine **1** (100 μM in CH_3CN) in the presence of $Cu(ClO_4)_2{\cdot}6H_2O$ (50 μM) and an increasing amount of Bu_4NOAc (0 μM, a; 37.5 μM, b; 87.5 μM, c; 125 μM, d). The first and last spectra of each experiment are coded blue and red, respectively.

same conditions, was also chlorinated to **1**-Me-Cl (Scheme 5c). On the contrary, replacing $Cu(ClO_4)_2{\cdot}6H_2O$ with $Cu(OAc)_2{\cdot}H_2O$ only led to the dehydrogenation of **1** (Scheme 5b), whereas no reaction occurred with **1**-Me (Scheme 5d). These data substantiated the hypothesis that $Cu(ClO_4)_2{\cdot}6H_2O$ oxidized the anilinyl moiety in compound **1** by single-electron transfer and that acetate attenuated the ability of copper(II) as a single-electron oxidant.

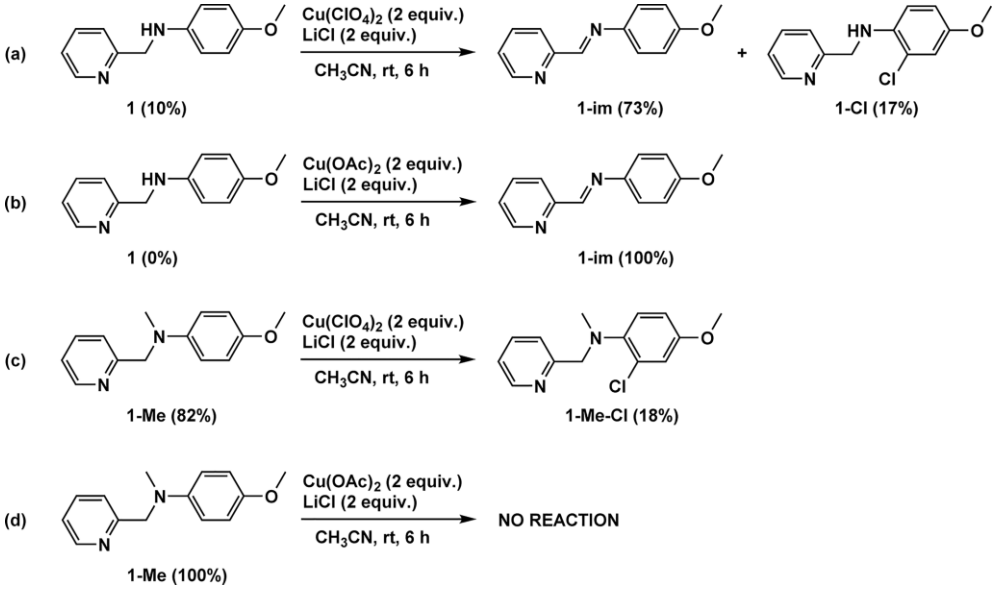

Scheme 5. $Cu(ClO_4)_2$ versus $Cu(OAc)_2$ in the oxidation of chelating amines **1** and **1**-Me. The copper salt (2.0 mol-equiv.), LiCl (2.0 mol-equiv.), CH_3CN (4 mL), and the amine (0.08 mmol) were added to a flask in this order. The resulting mixture was stirred at r.t. for 6 h. The reaction was then quenched by adding an EDTA solution (0.1 M, 5 mL, pH > 10), and the mixture was extracted with CH_2Cl_2 (2 × 5.0 mL). The combined organic layers were dried with anhydrous Na_2SO_4, filtered, and concentrated under reduced pressure. The crude mixture was analyzed by ^1H NMR spectroscopy ($CDCl_3$, 500 MHz). The molar percentages of identified compounds are included in parentheses.

© 2016 Wiley-VCH Verlag GmbH & Co. KGaA, Weinheim

Mechanistic Model

On the basis of these data, a catalytic cycle is sketched (Scheme 6). Chelating aromatic secondary amine **#** first replaces water in $[Cu_2(OAc)_4(H_2O)_2]$ to afford **A**. Acetate counterions in complex **A** act as an internal base to deprotonate the amino group to afford copper(II) amido complex **B** (i.e., "concerted metalation deprotonation"[36d]), in which the amine binds in a bidentate manner, as supported by the chemospecificity of chelating amines. Complex **A** also equilibrates with its off-cycle monomeric form **A′**, which is the resting state of the catalyst.[44] Base-promoted C–H bond cleavage in in-cycle complex **B** reduces the dicopper(II) core to dicopper(I) intermediate **C**, which may or may not traverse disproportionated intermediate **B′**.[45] The close contact between two copper(II) ions in **B**, which

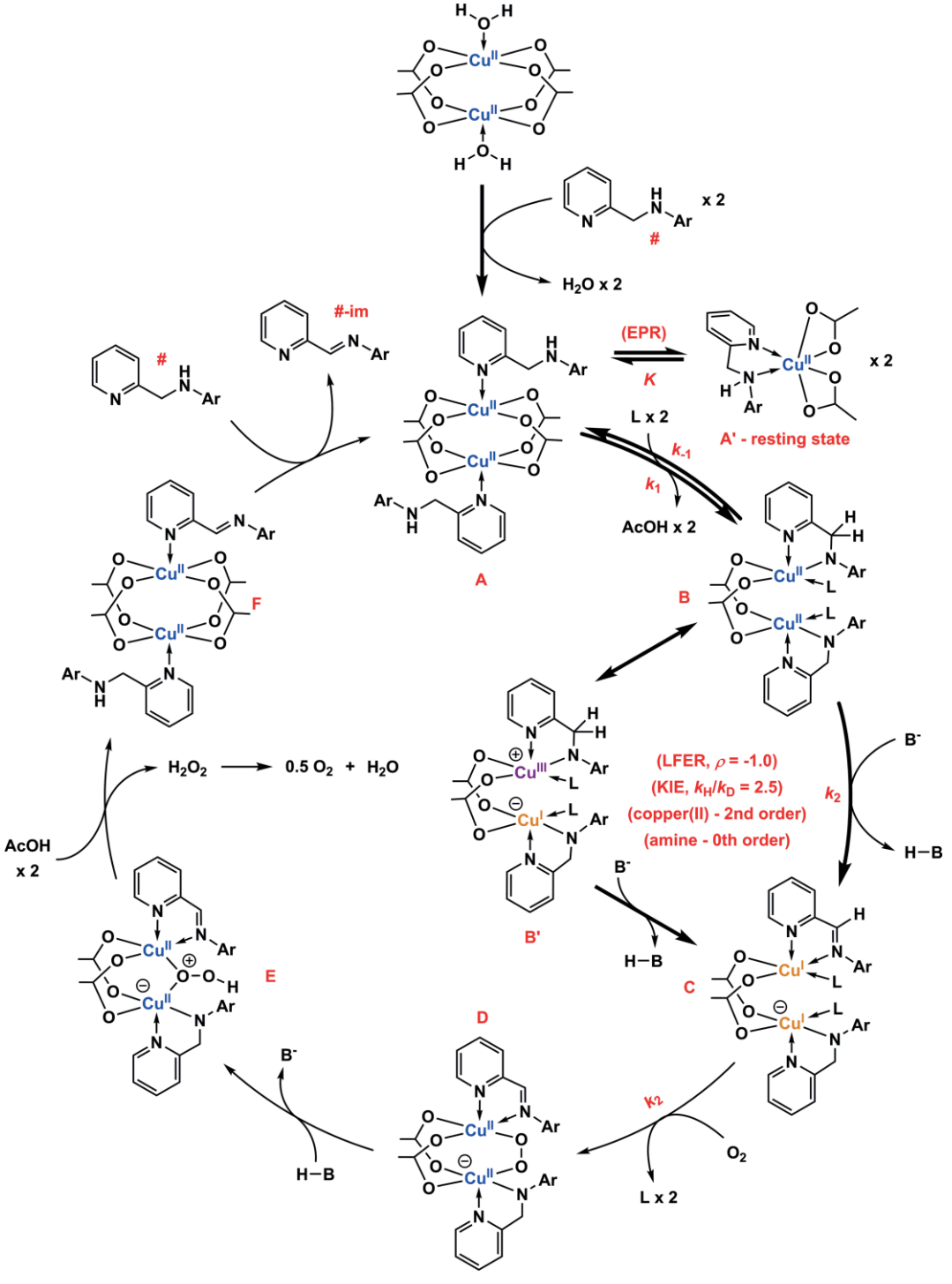

Scheme 6. Dinuclear catalytic cycle. Evidence supporting the individual steps is noted in parentheses. All steps are balanced. Copper is color-coded for its oxidation states: orange: +1; blue: +2; purple: +3. L is a monodentate ligand, such as CH_3CN or monodentate acetate. B = acetate or DBU. Cu–O (acetate) bond counts for a half bond (see footnote of Scheme 2).

© 2016 Wiley-VCH Verlag GmbH & Co. KGaA, Weinheim

should be similar to that in the copper(II) acetate dimers {e.g., d_{Cu-Cu} in $[Cu_2(\mathbf{6}\text{-Me})_2(OAc)_4]$ (Figure 3a) is 2.644(1) Å}, shall facilitate the two-electron transfer step. A recent computational study on the mechanism of a $Cu(OAc)_2$-mediated C–H functionalization reaction supports the beneficial ligand effect of acetate in lowering the transition-state energy for the disproportionation step within an acetate-supported dicopper(II) core.[46] The "redox cooperation" between two interacting metal centers separated by a short distance[47] is also cited in dipalladium catalysis.[10,48] This situation is different from another case of amine oxidation by a copper(II) complex, in which the shortest Cu–Cu distance is >7 Å and, hence, is less likely to have productive copper/copper interactions in aiding two-electron transfer.[38]

In the absence of O_2, $Cu(OAc)_2{\cdot}H_2O$ becomes the stoichiometric oxidant [Equation (1)]. The rate of the reaction is lowered as $Cu(OAc)_2{\cdot}H_2O$ is consumed. Under aerobic conditions, O_2 shall trap **C** (Scheme 6) to regenerate copper(II) in the form of μ-peroxo dicopper(II) species **D** and with subsequent steps turns the process catalytic in $Cu(OAc)_2{\cdot}H_2O$. Complex **D** may undergo stepwise protonation possibly through **E**[49] to afford complex **F** with the release of H_2O_2.[50] H_2O_2 rapidly disproportionates to O_2 and H_2O under copper-catalyzed conditions,[51] which accounts for the observed 2:1 (amine/O_2) stoichiometry. Substrate turnover converts complex **F** back into **A**. The turnover-limiting step is C–H bond cleavage of the substrate, which in effect is the oxidation of the amine at the expense of the reduction of the dicopper(II) core. This conclusion is supported by both the primary KIE (k_H/k_D = 2.5) and LFER (ϱ = –1.0) data. The steps after **C** are kinetically invisible and, therefore, are proposed on the basis of precedented chemistry. $Cu(OAc)_2{\cdot}H_2O$ is the catalyst, whereas O_2 is the stoichiometric oxidant for catalyst regeneration [Equation (2)]. This scenario is consistent with the "oxidase" model summarized by Stahl and co-workers.[3d,7a] Unlike Equation (1), there is no net production of AcOH if O_2 drives the cycle.

$$H_2im + 2\ Cu(OAc)_2 \rightarrow im + 2\ Cu(OAc) + 2\ AcOH \quad (1)$$

$$H_2im + 1/2\ O_2 \xrightarrow{Cu(OAc)_2} im + H_2O \quad (2)$$

The rate law of the conversion from **A** into **C** (bolded steps in Scheme 6) was derived [Equation (3)] by assuming that a steady state was reached at intermediate **B**. Further derivation to relate the rate to the concentrations of copper(II) and the acetate ions required the following approximations: (1) The equilibrium between **A** and **A′** [Equation (4)] favors mononuclear **A′**, as suggested by the EPR data, on the basis of which we approximated [**A′**] to the total copper(II) concentration $[Cu^{II}]_t$ [Equation (5)]. (2) The equilibrium constant K (see Scheme 6) shall depend on the concentration of a bidentate ligand [acetate in this case, Equation (6)], which would facilitate the formation of dimer **A**. (3) The base to deprotonate complex **B** is the acetate counterion [Equation (7)]. Acceptance of these approximations resulted in the rate law [Equation (8)] on which the following conclusions were drawn:

(1) Under anaerobic conditions, the rate of the reaction would drop as the reaction proceeds, because $[Cu^{II}]_t$ would decrease and [AcOH] would increase [Equation (8)]. The participation of O_2 leads to the regeneration of copper(II) in intermediate **D** and the consumption of AcOH in the H_2O_2 disproportionation step to maintain constant values of $[Cu^{II}]_t$ and [AcOH] and, therefore, maximizes the rate. (2) The reaction is second order in $[Cu^{II}]_t$. (3) If one (x = 1) bidentate acetate is required for the formation of dinuclear intermediates, the kinetic dependence on acetate is between first and second order, depending on the relative magnitude of the [AcOH] term in the denominator of Equation (8).

$$\frac{d[P]}{dt} = \frac{k_1k_2[\mathbf{A}][L]^2[base]}{k_{-1}[AcOH]^2 + k_2[base]} \quad (3)$$

$$[\mathbf{A}] = K[\mathbf{A'}]^2 \quad (4)$$

$$[\mathbf{A'}] \approx [Cu^{II}]_t \quad (5)$$

$$K = K'[AcO^-]^x;\ x \geq 1 \quad (6)$$

$$[base] = [AcO^-] \quad (7)$$

$$\frac{d[P]}{dt} = \frac{k_1k_2K'[Cu^{II}]_t^2[L]^2[AcO^-]^{x+1}}{k_{-1}[AcOH]^2 + k_2[AcO^-]};\ x \geq 1 \quad (8)$$

P = product imine; L = monodentate ligand (e.g., CH_3CN or monodentate acetate); k_1, k_2, and k_{-1} are marked on Scheme 6.

The Dual Role of Acetate as a Base and a Bridging Ligand

Acetate acts as the base in the reaction and the bridging bidentate ligand for facilitating the formation of dicopper intermediates. Both functions are factored into the rate law [Equation (8)]. To separate the functions of acetate as a base or a bridging ligand, 1,8-diazabicyclo[5.4.0]undec-7-ene (DBU), the conjugate acid of which has a pK_a of 24.1 in CH_3CN,[52] slightly larger than that of acetate (23.5),[53] was examined as a surrogate base for acetate. At a 40 mol-% loading of $Cu(ClO_4)_2{\cdot}6H_2O$ (relative to the amount of amine **1**), which is a mononuclear copper(II) source with little copper(II)/counterion interaction, in the presence of increasing amounts of DBU, the reaction proceeded at a slow rate and stalled once DBU reached 2 mol-equiv. relative to the amount of $Cu(ClO_4)_2{\cdot}6H_2O$ (Figure 9, filled blue squares). Acetate achieved a much higher rate at a high molar ratio (filled red squares), for example, 3:1 relative to the amount of copper(II). Furthermore, the rate was fitted as a quadratic function of $[AcO^-]$, which suggests second-order dependence.

© 2016 Wiley-VCH Verlag GmbH & Co. KGaA, Weinheim

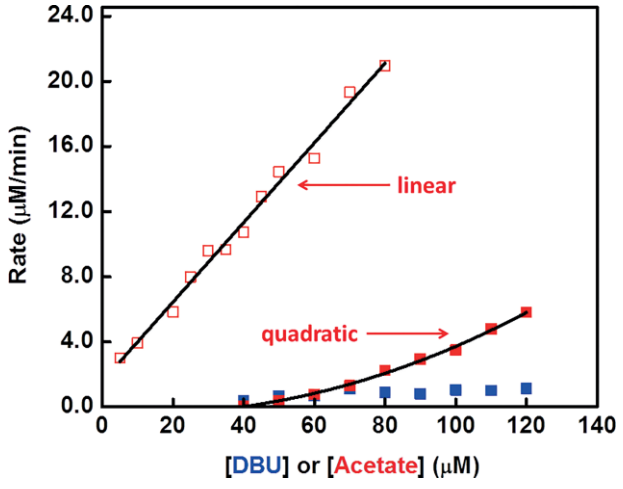

Figure 9. Rate of dehydrogenation of **1** (100 μM) in CH_3CN in the presence of $Cu(ClO_4)_2{\cdot}6H_2O$ (40 μM) and increasing amounts of DBU (blue filled squares), Bu_4NOAc alone (red filled squares), and Bu_4NOAc in the presence of 80 μM of DBU (red open squares).

What was most intriguing was the mutually beneficial effect of acetate and DBU, the combination of which enabled a much faster reaction than either could manage alone. At 80 mol-% loading of DBU (relative to the amount of amine **1**), the rate of the reaction increased linearly with growing concentrations of AcO^- (Figure 9, open red squares). Therefore, the reaction order of acetate was reduced to first order with 80 mol-% DBU present. It appears that DBU relieves acetate of the duty as a base, the remaining function of which is to facilitate the formation of dinuclear intermediates as a bridging ligand. Under the same conditions, for which both acetate and DBU were included, the kinetic order of $Cu(ClO_4)_2{\cdot}6H_2O$ was determined once again to be second order (1.9, Figure 7d), which further supports a dinuclear, rather than a mononuclear, pathway.

The function of acetate in copper(II) acetate mediated reactions has been scrutinized in two recent cases. Chemler and co-workers investigated the function of added acetate in the copper(II) carboxylate catalyzed aminooxygenation of olefins (Scheme 7a).[54] 2,2,6,6-Tetramethylpiperidin-1-oxyl (TEMPO) was found to promote the reaction, which suggested a radical-involved mechanism. The reaction exhibited half-order dependence on copper(II) carboxylate, which supported a dinuclear

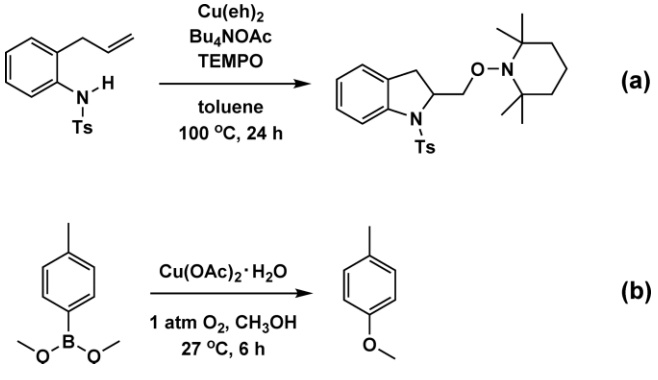

Scheme 7. Two other kinetically characterized $Cu(OAc)_2$-mediated reactions. eh = 2-ethylhexanoate, a soluble acetate surrogate.

resting state and a mononuclear active state of the copper catalyst.[55] Different from the rate dependence on acetate of the reaction described in this paper (Figure 9), at high concentrations of acetate, the aminooxygenation reaction was inhibited.[54] The authors concluded that the function of added acetate (in the form of Bu_4NOAc) was to activate the dinuclear copper(II) carboxylate to the active monomeric species. The carboxylate counterion and/or the added acetate also acted as a base for the formation of a copper(II) amido intermediate.

In the copper(II) acetate catalyzed Chan–Evans–Lam oxidative coupling reaction studied by Stahl and co-workers (Scheme 7b),[30] the reaction was either half or first order in copper(II), depending on the conditions.[56] Acetate appeared to facilitate the transmetalation step by interacting with the boron center and to deprotonate the nucleophile methanol, which also doubled as the solvent.[56] The addition of acetate beyond an optimal ratio of copper and acetate inhibited the reaction. The contrasting observations regarding acetate in the two reactions in Scheme 7 and our current case underscore the versatility of copper(II) acetate in mediating oxidation reactions and caution us from drawing overreaching conclusions on the mechanistic issues of copper catalysis and counterion effects.[57,40a,40b,44c,44d,58]

The extra benefit of including DBU is the elimination of the formation of **1**-im-OH. Because the inclusion of DBU did not alter the stoichiometry of O_2 consumption (Figure S9b), it is likely that (1) DBU accelerates the disproportionation of H_2O_2 or the copper(II)-bound hydroperoxo moiety,[59] which thus prevents the copper(II) catalyst from poisoning by the formation of **1**-im-OH, or (2) DBU disrupts the formation of electrophilic dicopper/O_2 complexes. In the presence of DBU, full conversion of **1** into **1**-im was achieved in the presence of 10 mol-% $Cu(ClO_4)_2{\cdot}6H_2O$ and 30 mol-% Bu_4NOAc (Figure 10), which renders this reaction a true catalytic process.

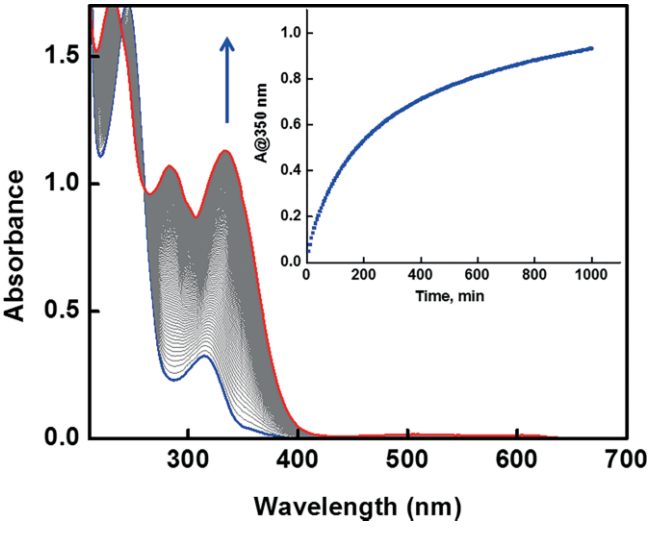

Figure 10. Absorption spectra of **1** (100 μM) in the presence of DBU (80 μM), $Cu(ClO_4)_2{\cdot}6H_2O$ (10 μM), and Bu_4NOAc (30 μM). Spectra were recorded at every 5 min. Inset shows variation in the absorbance at 350 nm versus time. The reaction mixture was stirred at a constant speed in the cuvette.

© 2016 Wiley-VCH Verlag GmbH & Co. KGaA, Weinheim

Conclusions

Copper(II) acetate catalyzes the aerobic dehydrogenation of chelating aromatic secondary amines. In addition to acting as a base, acetate aids the two-electron transfer elementary steps by facilitating the formation of dicopper species containing a short Cu–Cu distance (ca. 2.6 Å). Copper(II) acetate, therefore, is a simple dinuclear copper catalyst for two-electron transfer reactions of suitably selected substrates. Copper(II) acetate catalyzed dehydrogenation reactions with O_2 as the stoichiometric oxidant appeared in the literature more than half a century ago.[60] The importance of the dicopper(II) core of copper(II) acetate in dehydrogenation reactions was postulated at the beginning of this century.[61] The current work has provided credence to the hypothesis that copper(II) acetate is capable of mediating two-electron transfer steps in dehydrogenation and perhaps in oxidative coupling and C–H functionalization reactions, in which the acetate counterion may function as a base, a bridging ligand of a dinuclear catalyst, or both. This proposition shall be challenged experimentally and computationally under the contexts of other reactions.[62] The copper(II) acetate catalyzed dehydrogenation of a chelating aromatic secondary amine and the following arene hydroxylation may represent a simple functional model for both copper-dependent oxidases and oxygenases, which in its own right merits further investigations.[63]

Experimental Section

Materials and General Methods: Reagents and solvents were purchased from various commercial sources and were used without further purification unless otherwise stated. The purity of $Cu(OAc)_2{\cdot}H_2O$ was >99 %. Analytical thin-layer chromatography (TLC) was performed by using TLC plates precoated with silica gel 60 F254. Flash column chromatography was performed by using 40–63 μm (230–400 mesh) silica gel as the stationary phase. Silica gel was carefully flame-dried under vacuum to remove adsorbed moisture before use. ^1H and ^{13}C NMR spectra were recorded at 300 and 75 MHz or 500 and 125 MHz, respectively. All chemical shifts are reported in δ units relative to tetramethylsilane. High-resolution mass spectra were obtained by using a time-of-flight analyzer. Compounds **1**,[64] **3**,[65] **4**,[66] **5**,[67] **7**,[64a,68] and **9**[66,69] are known.

Synthesis and Characterization of New Compounds

1-Me: 4-Methoxy-*N*-methylaniline (200 mg, 1.46 mmol), 2-(chloromethyl)pyridine hydrochloride (240 mg, 1.46 mmol), and hexadecyltrimethylammonium chloride (HDTAC) (50 mg) were added to an aqueous NaOH solution (7 mL, 5 M), and the mixture was stirred at r.t. for 12 h. The mixture was diluted with water (100 mL) and extracted with CH_2Cl_2 (3 × 20 mL). The organic layer was dried with anhydrous Na_2SO_4, and subsequently, the solvent was removed under reduced pressure. The crude product was subjected to column chromatography (silica gel, 0–10 % EtOAc/CH_2Cl_2). The product was isolated as a pale-brown solid. The yield was 210 mg (63 %). ^1H NMR (300 MHz, $CDCl_3$): δ = 8.57 (d, J = 4.2 Hz, 1 H), 7.62 (dt, J = 7.2, 1.2 Hz, 1 H), 7.25 (d, J = 7.8 Hz, 1 H), 7.18 (t, J = 7.2 Hz, 1 H), 6.81 (d, J = 9.0 Hz, 2 H), 6.72 (d, J = 9.0 Hz, 2 H), 4.58 (s, 2 H), 3.74 (s, 3 H), 3.04 (s, 3 H) ppm. ^{13}C NMR (75 MHz, $CDCl_3$): δ = 159.7, 151.9, 149.5, 144.3, 136.8, 121.9, 121.2, 114.9, 114.2, 60.0, 55.8, 39.8 ppm. HRMS (EI+): calcd. for $C_{14}H_{16}N_2O$ 228.1263 $[M]^+$; found 228.1275.

2: Synthesized by a procedure similar to that described for **1**-Me. 4-(Chloromethyl)pyridine hydrochloride (500 mg, 3.04 mmol) and *p*-anisidine (450 mg, 3.65 mmol) were used. The crude product was subjected to column chromatography (silica gel, 0–50 % EtOAc/CH_2Cl_2). The product was isolated as an off-white solid. The yield was 384 mg (59 %). ^1H NMR (300 MHz, $CDCl_3$): δ = 8.54 (d, J = 5.4 Hz, 2 H), 7.29 (d, J = 5.4 Hz, 2 H), 6.75 (d, J = 9.0 Hz, 2 H), 6.54 (d, J = 9.0 Hz, 2 H), 4.43 (s, 2 H), 3.96 (br. s, 1 H), 3.73 (s, 3 H) ppm. ^{13}C NMR (125 MHz, $CDCl_3$): δ = 152.5, 149.9, 149.5, 141.7, 122.3, 115.1, 114.2, 55.8, 48.0 ppm. HRMS (EI+): calcd. for $C_{13}H_{14}N_2O$ 214.1106 $[M]^+$; found 214.1119.

6: A mixture of 2-pyridinecarbaldehyde (100 mg, 0.93 mmol) and 4-aminobiphenyl (157 mg, 0.93 mmol) was heated at reflux in dry toluene for 1 h. The solvent was removed under reduced pressure to afford the crude product, which was dissolved in CH_3OH/CH_2Cl_2 [2:8 (v/v), 10 mL] and cooled in an ice bath. $NaBH_4$ (52 mg, 1.39 mmol) was added in two batches between an interval of 30 min. After the complete addition of $NaBH_4$, the mixture was stirred for an additional 2 h. It was then diluted with water (100 mL) and extracted with CH_2Cl_2 (3 × 20 mL). The organic layer was separated and dried with anhydrous Na_2SO_4. The solvent was removed under reduced pressure, and the crude product was subjected to column chromatography (silica gel, 0–10 % EtOAc/CH_2Cl_2). The product was isolated as a pale-yellow solid. The yield was 169 mg (70 %). ^1H NMR (300 MHz, $CDCl_3$): δ = 8.60 (d, J = 4.2 Hz, 1 H), 7.66 (dt, J = 7.8, 1.8 Hz,1 H), 7.16–7.48 (m, 9 H), 6.74 (d, J = 9.0 Hz, 2 H), 4.92 (br. s, 1 H), 4.51 (s, 2 H) ppm. ^{13}C NMR (125 MHz, $CDCl_3$): δ = 158.4, 149.3, 147.4, 141.2, 136.7, 130.4, 127.9, 126.3, 126.2, 122.2, 121.6, 113.4, 49.3 ppm. HRMS (EI+): calcd. for $C_{18}H_{16}N_2$ 260.1313 $[M]^+$; found 260.1304.

6-Me: Compound **6** (100 mg, 0.38 mmol) was dissolved in dry THF (10 mL) and cooled in an ice bath. *t*BuOK (64 mg, 0.57 mmol) was added, and the mixture was stirred for 10 min. Iodomethane (0.1 mL) was added, and the mixture was stirred for 12 h. Then, the mixture was diluted with water (100 mL) and extracted with CH_2Cl_2 (3 × 20 mL). The organic layer was dried with anhydrous Na_2SO_4, and the solvent was subsequently removed under reduced pressure. The crude product was subjected to column chromatography (silica gel, 0–20 % EtOAc/CH_2Cl_2). The product was isolated as an off-white solid. The yield was 86 mg (82 %). ^1H NMR (500 MHz, $CDCl_3$): δ = 8.61 (d, J = 4.2 Hz, 1 H), 7.61 (dt, J = 7.8, 1.8 Hz, 1 H), 7.55 (dd, J = 8.4, 1.2 Hz, 2 H), 7.48 (dd, J = 9.0. 2.4 Hz, 2 H), 7.39 (t, J = 7.2 Hz, 2 H), 7.15–7.28 (m, 3 H), 6.78 (d, J = 9.0 Hz, 2 H), 4.71 (s, 2 H), 3.18 (s, 3 H) ppm. ^{13}C NMR (125 MHz, $CDCl_3$): δ = 159.2, 149.6, 148.6, 141.1, 136.9, 129.4, 128.7, 127.9, 126.3, 126.1, 122.0, 120.8, 112.5, 58.8, 39.2 ppm. HRMS (EI+): calcd. for $C_{19}H_{18}N_2$ 274.1470 $[M]^+$; found 274.1473.

8: Synthesized according to a procedure similar to that described for **1**-Me. 2-(Chloromethyl)pyridine hydrochloride (554 mg, 3.37 mmol) and 4-fluoroaniline (500 mg, 4.49 mmol) were used. The mixture was diluted by the addition of water (100 mL) and extracted with CH_2Cl_2 (3 × 20 mL). The organic layer was dried with anhydrous Na_2SO_4, and the solvent was removed under reduced pressure. The crude product was subjected to column chromatography (silica gel, 0–50 % EtOAc/CH_2Cl_2). The product was isolated as a white solid. The yield was 381 mg (42 %). ^1H NMR (300 MHz, $CDCl_3$): δ = 8.58 (d, J = 4.2 Hz, 1 H), 7.65 (dt, J = 7.8, 1.8 Hz, 1 H), 7.32 (d, J = 7.8 Hz, 1 H), 7.19 (t, J = 5.4 Hz, 1 H), 6.85–6.91 (m, 2 H), 6.57–6.63 (m, 2 H), 4.67 (br. s, 1 H), 4.41 (d, J = 5.4 Hz, 2 H) ppm. ^{13}C NMR (125 MHz, $CDCl_3$): δ = 158.4, 155.9 [d, $J(^{13}C,^{19}F)$ = 233 Hz], 149.3, 144.4, 136.8, 122.3, 121.8, 115.7 [d, $J(^{13}C,^{19}F)$ = 22 Hz], 113.9 [d, $J(^{13}C,^{19}F)$ = 7.0 Hz], 49.9 ppm. HRMS (EI+): calcd. for $C_{12}H_{11}FN_2$ 202.0906 $[M]^+$; found 202.0921.

© 2016 Wiley-VCH Verlag GmbH & Co. KGaA, Weinheim

10: Synthesized according to a procedure similar to that described for **6**. 4-Aminobenzonitrile (110 mg, 0.93 mmol) was used instead of 4-aminobiphenyl. The product was isolated as a white solid. The yield was 132 mg (68 %). ^{1}H NMR (300 MHz, $CDCl_3$): δ = 8.59 (d, J = 4.2 Hz, 1 H), 7.68 (dt, J = 7.8, 1.8 Hz, 1 H), 7.43 (d, J = 9.0 Hz, 2 H), 7.23–7.42 (m, 2 H), 6.64 (d, J = 8.4 Hz, 2 H), 5.56 (br. s, 1 H), 4.47 (d, J = 4.8 Hz, 2 H) ppm. ^{13}C NMR (125 MHz, $CDCl_3$): δ = 156.5, 151.1, 149.4, 137.1, 133.9, 122.8, 121.9, 120.6, 112.8, 99.2, 48.2 ppm. HRMS (EI+): calcd. for $C_{13}H_{11}N_3$ 209.0953 $[M]^+$; found 209.0958.

12: 2-Pyridinecarbonitrile (250 mg, 2.40 mmol) was dissolved in dry toluene (10 mL) in a round-bottom flask under argon. Methylmagnesium iodide (3.0 mL) was added, and the mixture was heated at reflux for 12 h. The mixture was cooled in an ice bath, and water (1 mL) was carefully added; the mixture was stirred for 10 min. The mixture was diluted with water (50 mL) and extracted with CH_2Cl_2 (3 × 20 mL). The organic layer was collected and dried with anhydrous Na_2SO_4. The solvent was removed under reduced pressure. The product was isolated as a pale-brown solid (185 mg, 57 %) (Scheme 8). ^{1}H NMR (300 MHz, $CDCl_3$): δ = 8.55 (d, J = 4.2 Hz, 1 H),7.63 (dt, J = 7.8, 1.8 Hz, 1 H), 7.44 (d, J = 7.8 Hz, 1 H), 7.12 (dt, J = 4.8, 1.2 Hz, 1 H), 2.3 (br. s, 2 H), 1.52 (s, 6 H) ppm. ^{13}C NMR (125 MHz, $CDCl_3$): δ = 168.2, 148.8, 136.6, 121.4, 118.5, 54.2, 31.3 ppm. HRMS (ESI+): calcd. for $C_8H_{13}N_2$137.1079 $[M + H]^+$; found 137.1090.

11: Compound **12** (30 mg, 0.22 mmol), (4-methylphenyl)boronic acid (45 mg, 0.33 mmol), pyridine (52 mg, 0.66 mmol), and $Cu(OAc)_2{\cdot}H_2O$ (44 mg, 0.22 mg) were dissolved in CH_3CN (8 mL), and the mixture was stirred at r.t. for 12 h. A basic EDTA solution (5 mL, 0.1 M, pH 10) was added, and the mixture was stirred for 10 min. The mixture was then extracted with CH_2Cl_2 (2 × 10 mL). The organic layer was collected and dried with anhydrous Na_2SO_4. The solvent was removed under reduced pressure. The crude product was subjected to column chromatography (silica gel, 0–30 % EtOAc/CH_2Cl_2). The product was isolated as a pale-brown solid. The yield was 31 mg (62 %) (Scheme 8). ^{1}H NMR (500 MHz, $CDCl_3$): δ = 8.60 (d, J = 4.8 Hz, 1 H),7.59 (d, J = 4.2 Hz, 1 H), 7.13 (q, J = 4.4 Hz, 1 H), 6.85 (d, J = 8.2 Hz, 2 H), 6.25 (d, J = 8.2 Hz, 2 H), 4.13 (br. s, 1 H), 2.2 (s, 3 H), 1.67 (s, 6 H) ppm. ^{13}C NMR (125 MHz, $CDCl_3$): δ = 166.4, 148.9, 143.6, 136.9, 129.5, 126.8, 121.6, 120.9, 115.9, 57.9, 29.3, 20.5 ppm. HRMS (ESI+): calcd. for $C_{15}H_{18}N_2Na$ 249.1368 $[M + Na]^+$; found 249.1377.

***N*-(4-Isopropylphenyl)-1-(pyridin-2-yl)methanimine (13):** A mixture of 2-pyridinecarbaldehyde (500 mg, 4.66 mmol) and 4-isopropylaniline (631 mg, 4.66 mmol) was heated at reflux in toluene (10 mL) for 1 h. The solvent was removed under reduced pressure, and the obtained residue was purified by precipitation from CH_2Cl_2/hexanes. The product was isolated as an off-white solid. The yield was 857 mg (82 %). ^{1}H NMR (300 MHz, $CDCl_3$): δ = 8.69 (d, J = 4.8 Hz, 1 H), 8.62 (s, 1 H), 8.19 (d, J = 7.8 Hz, 1 H), 7.78 (t, J = 7.8 Hz, 1 H), 7.32–7.35 (m, 1 H), 7.22–7.29 (m, 4 H), 2.93 (sept, J = 6.6 Hz, 1 H), 1.27 (s, 3 H), 1.25 (s, 3 H) ppm. ^{13}C NMR (75 MHz, $CDCl_3$): δ = 159.7, 154.8, 149.7, 148.6, 147.8, 136.6, 127.3, 125.0, 121.8, 121.3, 33.8, 24.1 ppm. HRMS (ESI+): calcd. for $C_{15}H_{17}N_2$ 225.1392 $[M + H]^+$; found 225.1394. This compound is the imine precursor for the amine (next compound) used for LFER studies.

(2-Pyridylmethyl)(4-isopropylphenyl)amine (14): *N*-(4-Isopropylphenyl)-1-(pyridin-2-yl)methanimine (100 mg, 0.44 mmol) was dissolved in CH_2Cl_2/CH_3OH (8:2) and cooled in an ice bath. $NaBH_4$ (25 mg, 0.67 mmol) was added, and the mixture was stirred for an additional 2 h. It was then diluted with water (100 mL) and extracted with CH_2Cl_2 (3 × 20 mL). The organic layer was separated and dried with anhydrous Na_2SO_4. The solvent was removed under reduced pressure, and the crude product was subjected to column chromatography (silica gel, 0–10 % EtOAc/CH_2Cl_2). The yield was 72 mg (71 %). ^{1}H NMR (300 MHz, $CDCl_3$): δ = 8.58 (d, J = 4.8 Hz, 1 H), 7.64 (dt, J = 7.8, 1.8 Hz, 1 H), 7.35 (d, J = 7.8 Hz, 1 H), 7.18 (t, J = 4.8 Hz, 1 H), 7.05 (d, J = 8.4 Hz, 2 H), 6.62 (d, J = 9.0 Hz, 2 H), 4.45 (s, 2 H), 4.11 (br. s, 1 H), 2.80 (sept, J = 6.6 Hz, 1 H), 1.21 (s, 3 H), 1.19 (s, 3 H) ppm. ^{13}C NMR (75 MHz, $CDCl_3$): δ = 158.9, 149.2, 146.1, 138.1, 136.6, 127.2, 122.1, 121.6, 113.1, 49.7, 33.2, 24.3 ppm. HRMS (ESI+): calcd. for $C_{15}H_{19}N_2$ 227.1548 $[M + H]^+$; found 227.1538.

***N*-(4-Methoxyphenyl)-2-picolinamide (15):** 2-Picolinic acid (500 mg, 4.06 mmol) was dissolved in dry CH_2Cl_2 (10 mL). Oxalyl chloride (1.0 mL) was added, and the mixture was stirred at r.t. for 30 min. The solvent was removed under reduced pressure. The crude acyl chloride was then dissolved in dry CH_2Cl_2 (10 mL). Anhydrous Na_2CO_3 (860 mg, 8.12 mmol) and *p*-anisidine (500 mg, 4.06 mmol) were added sequentially, and mixture was stirred at r.t. After 12 h, the mixture was diluted with CH_2Cl_2 (50 mL) and washed with dilute HCl (2 % v/v, 20 mL). The organic layer was neutralized with a dilute $NaHCO_3$ solution. The organic layer was collected and dried with anhydrous Na_2SO_4, and the solvent was subsequently removed under reduced pressure. The crude product was subjected to column chromatography (silica gel, CH_2Cl_2) to afford the pure product. The product was isolated as a dull-white solid. The yield was 47 % (433 mg) (Scheme 9). ^{1}H NMR (300 MHz, $CDCl_3$): δ = 9.93 (br. s, 1 H), 8.61 (d, J = 4.8 Hz, 1 H), 8.30 (d, J = 7.8 Hz, 1 H), 7.90 (dt, J = 7.2, 1.2 Hz, 1 H), 7.70 (d, J = 9.0 Hz, 2 H), 7.47 (t, J = 7.8 Hz, 1 H), 6.93 (d, J = 9.0 Hz, 2 H), 3.82 (s, 3 H) ppm.[70]

1-d_2: Lithium aluminum deuteride ($LiAlD_4$) (36 mg, 0.86 mmol) was suspended in dry THF (10 mL) in a round-bottom flask (50 mL) under argon and cooled in an ice bath. *N*-(4-Methoxyphenyl)-2-picolinamide (100 mg, 0.44 mmol) in dry THF (2.0 mL) was added slowly, and the mixture was heated at reflux for 12 h. The mixture was then cooled in an ice bath, and the reaction was quenched by the addition of water (1.0 mL), which was followed by the addition of an NaOH solution (5 % v/v, 20 mL). It was extracted with CH_2Cl_2 (2 × 50 mL). The organic layer was collected and dried with anhydrous Na_2SO_4. The solvent was removed under reduced pressure, and the crude product was subjected to column chromatography (silica gel, 0–50 % EtOAc/CH_2Cl_2) to isolate the product. The product was isolated as pale-brown solid. The yield was 45 % (42 mg) (Scheme 9). ^{1}H NMR (300 MHz, $CDCl_3$): δ = 8.59 (d, J = 4.8 Hz, 1 H), 7.62 (t, J = 9.0 Hz, 1 H), 7.35 (dd, J = 6.6, 1.2 Hz, 1 H), 7.17–7.19 (m,

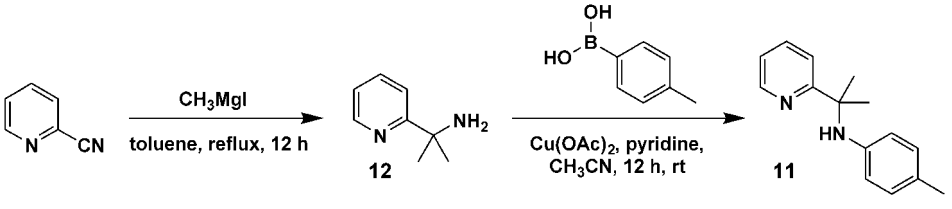

Scheme 8. Synthesis of **11**.

© 2016 Wiley-VCH Verlag GmbH & Co. KGaA, Weinheim

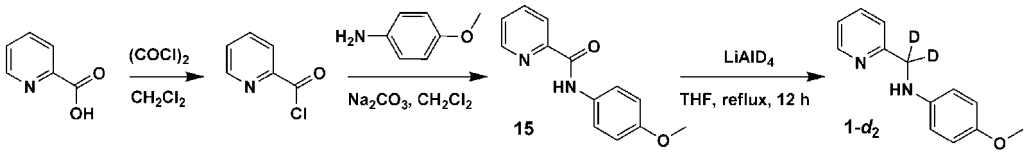

Scheme 9. Synthesis of **1**-d_2.

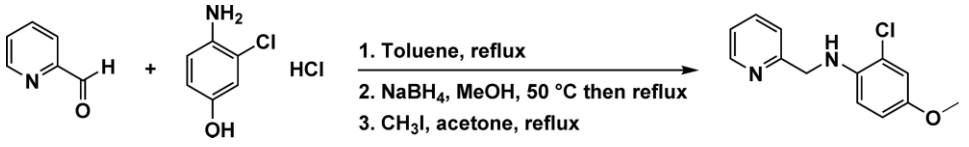

Scheme 10. Synthesis of **1**-Cl.

1 H), 6.78 (d, J = 9.0 Hz, 2 H), 6.63 (d, J = 9.0 Hz, 2 H), 3.73 (s, 3 H), 3.2 (br. s, 1 H) ppm. ^{13}C NMR (125 MHz, $CDCl_3$): δ = 158.8, 152.2, 149.3, 142.3, 136.7, 122.1, 121.7, 114.9, 114.3, 55.8, 49.6 [quint, $J(^{13}C,^{2}H)$ = 21.5 Hz] ppm. HRMS (ESI+): calcd. for $C_{13}H_{13}D_2N_2O$ 217.1309 $[M + H]^+$; found 217.1297.

1-Cl: A mixture of 2-pyridinecarbaldehyde (200 mg, 1.87 mmol) and 4-amino-3-chlorophenol hydrochloride (336 mg, 1.87 mmol) was heated at reflux in dry toluene (5 mL) for 1 h. The solvent was removed under reduced pressure to afford the crude product, which was dissolved in CH_3OH (8 mL). The solution was heated at 50 °C, and then $NaBH_4$ (120 mg, 3.17 mmol) was added. After the complete addition of $NaBH_4$, the mixture was heated at reflux for 30 min. To quench the reaction, water was added. Most of the CH_3OH was removed under reduced pressure, and then the aqueous solution was extracted with CH_2Cl_2. The organic layer was dried with anhydrous Na_2SO_4, filtered, and concentrated in vacuo. The resulting residue was dissolved in acetone (5 mL), and then K_2CO_3 (198 mg, 1.43 mmol) was added, followed by the addition of CH_3I (89 μL, 1.43 mmol). The mixture was heated at reflux for 3 h and then stirred at r.t. overnight. The crude mixture was concentrated in vacuo and then subjected to column chromatography (silica gel, 15 % EtOAc/hexanes) to afford the desired product as a yellow oil (Scheme 10). ^{1}H NMR (500 MHz, $CDCl_3$): δ = 8.60–8.57 (m, 1 H), 7.64 (dt, J = 12.0, 6.0 Hz, 1 H), 7.34–7.30 (m, 1 H), 7.20–7.16 (m, 1 H), 6.92 (d, J = 2.4 Hz, 1 H), 6.69 (dd, J = 9.0, 3.0 Hz, 1 H), 6.54 (d, J = 9.0 Hz, 1 H), 4.79 (s, 2 H), 3.72 (s, 3 H) ppm. ^{13}C NMR (125 MHz, $CDCl_3$): δ = 158.6, 151.7, 149.4, 138.3, 137.0, 122.3, 121.5, 120.0, 115.6, 113.8, 112.6, 56.1, 49.8 ppm. HRMS (ESI+): calcd. for $C_{13}H_{14}ClN_2O$ 249.0795 $[M + H]^+$; found 249.0785.

Reaction under Anaerobic Conditions: A solution of amine **1** (0.08 mmol) in CH_3CN (4.0 mL) was placed in a two-neck, round-bottom flask. This flask was fitted with a solid addition adapter and an argon-supplying adapter. $Cu(OAc)_2{\cdot}H_2O$ (0.08 mmol) was transferred to the solid addition adaptor. Through three freeze–pump–thaw cycles, the system was put under argon. Once the system was under argon, $Cu(OAc)_2{\cdot}H_2O$ (0.08 mmol) was added to the flask by rotating the adapter, and the reaction was allowed to run under constant stirring for 5 min. Afterwards, the reaction was quenched by addition of an EDTA solution (0.1 M, pH > 10, 5 mL). The resulting mixture was transferred into a separatory funnel and extracted with CH_2Cl_2 (2 × 5.0 mL). The combined organic layers were dried with anhydrous Na_2SO_4, filtered, and concentrated under reduced pressure. The crude mixture was analyzed by ^{1}H NMR spectroscopy ($CDCl_3$, 500 MHz) to determine the conversion value of the reaction (Table 1, Entry 5).

Electron Paramagnetic Resonance Measurements: Solution EPR spectra were measured at the X-band microwave frequency (9.4 GHz) by using a Bruker Elexsys-500 Spectrometer at r.t. The magnetic field was calibrated by using DPPH (2,2-diphenyl-1-picrylhydrazyl) standard (g = 2.0037), and the microwave frequency was measured by using a built-in digital counter. The modulation amplitude and microwave power were optimized for high signal/noise ratio. Glass capillary tubes were used as sample holders. In a typical measurement, a freshly prepared mixture was taken in a glass capillary (borosilicate melting point tube, i.d. ca. 1.4 mm) and then placed inside a standard quartz X-band sample tube. The background from the empty capillary tube was measured prior to each sample measurement and was subsequently subtracted. Sufficient care was taken to maintain similar experimental conditions during both the background and sample measurements.

Manometry: A round-bottom flask equipped with a magnetic stirring bar was connected to a computer-interfaced digital manometer (VWR Traceable manometer) through a T-bore stopcock and Teflon tubing. The amine solution in CH_3CN was added to the reaction vessel through the T-bore stopcock by using a syringe and allowed to equilibrate at r.t. Then, a CH_3CN solution of $Cu(OAc)_2{\cdot}H_2O$ was added through the syringe, and immediately the T-bore stopcock was turned to close the reaction vessel. The change in pressure with respect to time was monitored by using Data Acquisition Software (DASTM, Control Company).

Kinetic Measurements: CH_3CN stock solutions of amine (0.2 mM, 400 μL) and $Cu(OAc)_2{\cdot}H_2O$ (0.1 mM, 400 μL) were successively added by syringes into a semimicro quartz cuvette (1.5 mL). The combined solutions were mixed for ca. 10 s before absorption spectra were acquired. The spectroscopic data were collected at 22 °C every 2 min. The rate of the reaction was obtained from the slope of the linear portion immediately after mixing up to the 14 min mark. The absorption spectra of compounds **1** and **1**-im in their metal-free forms in CH_3CN are shown in Figure S10.

X-ray Crystallography: A suitable single crystal was mounted on a goniometer head of an APEX II diffractometer by using a nylon loop with a small amount of Paratone oil. All three samples were run at –170 °C with the first two at 60 s of frame time and the third at 40 s. For the first two, 0.5° Ω were employed, whereas the third was 0.3°. Data integration was performed by using the program SAINT, which is part of the Bruker suite of programs. Empirical absorption correction was performed by using SADABS. XPREP was used to obtain an indication of the space group, and the structure was solved by direct methods and refined by SHELXTL. With the excep-

© 2016 Wiley-VCH Verlag GmbH & Co. KGaA, Weinheim

tion noted below, all non-hydrogen atoms were refined anisotropically, whereas hydrogen atoms were typically placed in calculated positions and constrained to a riding model. $[Cu_2(OAc)_4(\mathbf{6}\text{-Me})_2]$ (Figure 3a) was needle-like and **8**-im-OH (Figure S4) was a thin sheet. Reflections were not found to adequately high angles in spite of the longer frame times nor was the data collection complete. Not surprisingly, the data/parameter ratio was generally not 10:1. Notwithstanding these problems, both structures make chemical sense, and only the fine details are in question. The dicopper(II) tetraacetate structure of $[Cu_2(OAc)_4(\mathbf{6}\text{-Me})_2]$ is quite normal if compared to the literature structures containing other axial ligands. In the structure of **8**-im-OH, electron density was found in the area between molecules and it was assigned as oxygen from a water molecule. It proved to be disordered and was refined as 1/2 of an oxygen atom at each site. CCDC 1455876 {for $[Cu_2(\mathbf{6\text{-Me}})_2(OAc)_4]$}, 1455877 {for [Cu(**11**)$(OAc)_2$]}, and 1455878 (for **8**-im-OH) contain the supplementary crystallographic data for this paper. These data can be obtained free of charge from The Cambridge Crystallographic Data Centre.

Acknowledgments

This work was supported by the National Science Foundation (CHE1213574) and the Florida State University Council on Research and Creativity.

Keywords: Amines · Bridging ligands · Copper · Dehydrogenation · Dinuclear catalysis · Oxidation

[1] a) G. Evano, N. Blanchard, M. Toumi, *Chem. Rev.* **2008**, *108*, 3054–3131; b) C. Zhang, C. Tang, N. Jiao, *Chem. Soc. Rev.* **2012**, *41*, 3464–3484; c) S. E. Allen, R. R. Walvoord, R. Padilla-Salinas, M. C. Kozlowski, *Chem. Rev.* **2013**, *113*, 6234–6458.

[2] a) J. Hartwig, *Organotransition Metal Chemistry – From Bonding to Catalysis*, University Science Books, Sausalito, CA, **2010**; b) S. S. Stahl, *Angew. Chem. Int. Ed.* **2004**, *43*, 3400–3420; *Angew. Chem.* **2004**, *116*, 3480–3501; c) T. W. Lyons, M. S. Sanford, *Chem. Rev.* **2010**, *110*, 1147–1169; d) C. C. C. Johansson Seechurn, M. O. Kitching, T. J. Colacot, V. Snieckus, *Angew. Chem. Int. Ed.* **2012**, *51*, 5062–5085; *Angew. Chem.* **2012**, *124*, 5150–5174; e) K. M. Engle, J.-Q. Yu, *J. Org. Chem.* **2013**, *78*, 8927–8955.

[3] a) T. Cohen, J. Wood, A. G. J. Dietz, *Tetrahedron Lett.* **1974**, *15*, 3555–3558; b) N. Yoshikai, E. Nakamura, *Chem. Rev.* **2012**, *112*, 2339–2372; c) A. Casitas, X. Ribas, *Chem. Sci.* **2013**, *4*, 2301–2318; d) S. D. McCann, S. S. Stahl, *Acc. Chem. Res.* **2015**, *48*, 1756–1766.

[4] a) E. Nakamura, S. Mori, *Angew. Chem. Int. Ed.* **2000**, *39*, 3750–3771; *Angew. Chem.* **2000**, *112*, 3902–3924; b) S. H. Bertz, R. A. Hardin, T. J. Heavey, C. A. Ogle, *Angew. Chem. Int. Ed.* **2013**, *52*, 10250–10252; *Angew. Chem.* **2013**, *125*, 10440–10442.

[5] a) A. Casitas, A. E. King, T. Parella, M. Costas, S. S. Stahl, X. Ribas, *Chem. Sci.* **2010**, *1*, 326–330; b) L. M. Huffman, A. Casitas, M. Font, M. Canta, M. Costas, X. Ribas, S. S. Stahl, *Chem. Eur. J.* **2011**, *17*, 10643–10650; c) M. Font, T. Parella, M. Costas, X. Ribas, *Organometallics* **2012**, *31*, 7976–7982; d) C. Sambiagio, S. P. Marsden, A. J. Blacker, P. C. McGowan, *Chem. Soc. Rev.* **2014**, *43*, 3525–3550.

[6] a) X. Ribas, D. A. Jackson, B. Donnadieu, J. Mahía, T. Parella, R. Xifra, B. Hedman, K. O. Hodgson, A. Llobet, T. D. P. Stack, *Angew. Chem. Int. Ed.* **2002**, *41*, 2991–2994; *Angew. Chem.* **2002**, *114*, 3117–3120; b) B. Yao, D.-X. Wang, Z.-T. Huang, M.-X. Wang, *Chem. Commun.* **2009**, 2899–2901; c) A. E. King, L. M. Huffman, A. Casitas, M. Costas, X. Ribas, S. S. Stahl, *J. Am. Chem. Soc.* **2010**, *132*, 12068–12073.

[7] a) A. E. Wendlandt, A. M. Suess, S. S. Stahl, *Angew. Chem. Int. Ed.* **2011**, *50*, 11062–11087; *Angew. Chem.* **2011**, *123*, 11256–11283; b) A. M. Suess, M. Z. Ertem, C. J. Cramer, S. S. Stahl, *J. Am. Chem. Soc.* **2013**, *135*, 9797–9804.

[8] a) H. Furuta, H. Maeda, A. Osuka, *J. Am. Chem. Soc.* **2000**, *122*, 803–807; b) B. Adinarayana, A. P. Thomas, C. H. Suresh, A. Srinivasan, *Angew. Chem. Int. Ed.* **2015**, *54*, 10478–10482; *Angew. Chem.* **2015**, *127*, 10624–10628.

[9] M. Melník, M. Kabešová, *J. Coord. Chem.* **2000**, *50*, 323–338.

[10] D. C. Powers, T. Ritter, *Acc. Chem. Res.* **2012**, *45*, 840–850.

[11] E. Tkatchouk, N. P. Mankad, D. Benitez, I. William, A. Goddard, F. D. Toste, *J. Am. Chem. Soc.* **2011**, *133*, 14293–14300.

[12] a) N. Kitajima, Y. Moro-oka, *Chem. Rev.* **1994**, *94*, 737–757; b) E. I. Solomon, U. M. Sundaram, T. E. Machonkin, *Chem. Rev.* **1996**, *96*, 2563–2605; c) E. I. Solomon, P. Chen, M. Metz, S.-K. Lee, A. E. Palmer, *Angew. Chem. Int. Ed.* **2001**, *40*, 4570–4590; *Angew. Chem.* **2001**, *113*, 4702–4724; d) K. D. Karlin, S. Itoh, *Reactive Intermediates in Chemistry and Biology*, vol. 4 (Ed.: S. E. Rokita), Wiley, Hoboken, NJ, **2011**; e) M. Rolff, J. Schottenheim, H. Decker, F. Tuczek, *Chem. Soc. Rev.* **2011**, *40*, 4077–4098.

[13] a) P. L. Holland, W. B. Tolman, *Coord. Chem. Rev.* **1999**, *190–192*, 855–869; b) E. A. Lewis, W. B. Tolman, *Chem. Rev.* **2004**, *104*, 1047–1076; c) E. Kim, E. E. Chufan, K. Kamaraj, K. D. Karlin, *Chem. Rev.* **2004**, *104*, 1077–1133; d) L. M. Mirica, X. Ottenwaelder, T. D. P. Stack, *Chem. Rev.* **2004**, *104*, 1013–1045; e) L. Q. Hatcher, K. D. Karlin, *J. Biol. Inorg. Chem.* **2004**, *9*, 669–683.

[14] X.-X. Guo, D.-W. Gu, Z. Wu, W. Zhang, *Chem. Rev.* **2015**, *115*, 1622–1651.

[15] G.-C. Kuang, P. M. Guha, W. S. Brotherton, J. T. Simmons, L. A. Stankee, B. T. Nguyen, R. J. Clark, L. Zhu, *J. Am. Chem. Soc.* **2011**, *133*, 13984–14001.

[16] P. Siemsen, R. C. Livingston, F. Diederich, *Angew. Chem. Int. Ed.* **2000**, *39*, 2632–2657; *Angew. Chem.* **2000**, *112*, 2740–2767.

[17] a) G. Zhang, H. Yi, G. Zhang, Y. Deng, R. Bai, H. Zhang, J. T. Miller, A. J. Kropf, E. E. Bunel, A. Lei, *J. Am. Chem. Soc.* **2014**, *136*, 924–926; b) R. Bai, G. Zhang, H. Yi, Z. Huang, X. Qi, C. Liu, J. T. Miller, A. J. Kropf, E. E. Bunel, Y. Lan, A. Lei, *J. Am. Chem. Soc.* **2014**, *136*, 16760–16763.

[18] a) J. E. Hein, V. V. Fokin, *Chem. Soc. Rev.* **2010**, *39*, 1302–1315; b) B. T. Worrell, J. A. Malik, V. V. Fokin, *Science* **2013**, *340*, 457–460; c) L. Jin, D. R. Tolentino, M. Melaimi, G. Bertrand, *Sci. Adv.* **2015**, *1*, e1500304.

[19] a) J. K. Kochi, R. V. Subramanian, *Inorg. Chem.* **1965**, *4*, 1527–1533; b) A. T. A. Cheng, R. A. Howald, *Inorg. Chem.* **1968**, *7*, 2100–2105; c) P. Sharrock, M. Melník, *Can. J. Chem.* **1985**, *63*, 52–56; d) Y. Fujii, N. Nakasuka, M. Tanaka, H. Yamada, M. Mizuta, *Inorg. Chem.* **1989**, *28*, 3600–3602.

[20] S. V. Ley, A. W. Thomas, *Angew. Chem. Int. Ed.* **2003**, *42*, 5400–5449; *Angew. Chem.* **2003**, *115*, 5558–5607.

[21] Copper(II) acetate may carry different roles, as exemplified by the two recently reported reactions shown in Scheme 7 and discussed in the accompanying section.

[22] Various synthetic methods have been reported for copper-mediated amine-to-imine or alcohol-to-imine oxidations (see ref.[23a–23g]); ref.[24] is an example of the copper(II) acetate catalyzed dehydrogenation of aminals.

[23] a) R. D. Patil, S. Adimurthy, *Adv. Synth. Catal.* **2011**, *353*, 1695–1700; b) T. Sonobe, K. Oisaki, M. Kanai, *Chem. Sci.* **2012**, *3*, 3249–3255; c) M. Largeron, M.-B. Fleury, *Angew. Chem. Int. Ed.* **2012**, *51*, 5409–5412; *Angew. Chem.* **2012**, *124*, 5505–5508; d) J. Kim, S. S. Stahl, *ACS Catal.* **2013**, *3*, 1652–1656; e) M. Largeron, M.-B. Fleury, *Chem. Eur. J.* **2015**, *21*, 3815–3820; f) W. Yin, C. Wang, Y. Huang, *Org. Lett.* **2013**, *15*, 1850–1853; g) H. Chen, Q. Wang, Y. Huang, *Tetrahedron* **2015**, *71*, 3632–3636.

[24] M. T. Richers, C. Zhao, D. Seidel, *Beilstein J. Org. Chem.* **2013**, *9*, 1194–1201.

[25] There is another mechanistically characterized case in which a copper catalyst mediates both dehydrogenation (dehydrogenative coupling) as the major reaction and oxygenation as a minor path; distinguished from the current work, the oxygenated minor product in the referenced study was postulated to be a cofactor in the major dehydrogenative coupling pathway with a different kinetic profile: J. B. Hewgley, S. S. Stahl, M. C. Kozlowski, *J. Am. Chem. Soc.* **2008**, *130*, 12232–12233.

[26] a) M. Kirchgessner, K. Sreenath, K. R. Gopidas, *J. Org. Chem.* **2006**, *71*, 9849–9852; b) K. Sreenath, C. V. Suneesh, V. K. R. Kumar, K. R. Gopidas, *J. Org. Chem.* **2008**, *73*, 3245–3251.

[27] The comparison of the reaction progress in a UV/Vis assay is shown in Figure S5. Whereas the ratio of initial rates (up to 10 min point) of **1**-im production under aerobic and anaerobic conditions was ca. 5-fold, the ratio of the **1**-im-OH production rate was ca. 13-fold. These data suggest that O_2 participates in the oxygenation reaction, rather than the acetate

 © 2016 Wiley-VCH Verlag GmbH & Co. KGaA, Weinheim

ions, as in an oxidative acetoxylation reaction. For examples of copper-catalyzed oxidative acetoxylation, see: a) Y. Takizawa, A. Tateishi, J. Sugiyama, H. Yoshida, N. Yoshihara, *J. Chem. Soc., Chem. Commun.* **1991**, 104–105; b) X. Chen, X.-S. Hao, C. E. Goodhue, J.-Q. Yu, *J. Am. Chem. Soc.* **2006**, *128*, 6790–6791; c) Z. Wang, Y. Kuninobu, M. Kanai, *Org. Lett.* **2014**, *16*, 4790–4793.

[28] a) H. R. Gersmann, J. D. Swalen, *J. Chem. Phys.* **1962**, *36*, 3221–3233; b) J. A. Weil, J. R. Bolton, J. E. Wertz, *Electron Paramagnetic Resonance – Elementary Theory and Practical Applications*, Wiley, New York, **1994**; c) R. Kannappan, R. Mahalakshmy, T. M. Rajendiran, R. Venkatesan, P. S. Rao, *J. Chem. Sci.* **2003**, *115*, 1–14.

[29] B. Bleaney, K. D. Bowers, *Proc. R. Soc. London, Ser. A* **1952**, *214*, 451–465.

[30] A. E. King, T. C. Brunold, S. S. Stahl, *J. Am. Chem. Soc.* **2009**, *131*, 5044–5045.

[31] M. Montalti, A. Credi, L. Prodi, M. T. Gandolfi, *Handbooks of Photochemistry*, 3rd ed., CRC Taylor & Francis, Boca Raton, FL, **2006**, pp. 624–628.

[32] The absorption spectra of independently prepared **1** and **1**-im are included in Figure S10.

[33] See more data in Table S3 and Figure S11.

[34] E. M. Simmons, J. F. Hartwig, *Angew. Chem. Int. Ed.* **2012**, *51*, 3066–3072; *Angew. Chem.* **2012**, *124*, 3120–3126.

[35] See time-dependent spectra in Figure S12.

[36] a) B. Biswas, M. Sugimoto, S. Sakaki, *Organometallics* **2000**, *19*, 3895–3908; b) D. L. Davies, S. M. A. Donald, S. A. Macgregor, *J. Am. Chem. Soc.* **2005**, *127*, 13754–13755; c) D. García-Cuadrado, A. A. C. Braga, F. Maseras, A. M. Echavarren, *J. Am. Chem. Soc.* **2006**, *128*, 1066–1067; d) H.-Y. Sun, S. I. Gorelsky, D. R. Stuart, L.-C. Campeau, K. Fagnou, *J. Org. Chem.* **2010**, *75*, 8180–8189.

[37] a) M. Nishino, K. Hirano, T. Satoh, M. Miura, *Angew. Chem. Int. Ed.* **2012**, *51*, 6993–6997; *Angew. Chem.* **2012**, *124*, 7099–7103; b) M. Nishino, K. Hirano, T. Satoh, M. Miura, *Angew. Chem. Int. Ed.* **2013**, *52*, 4457–4461; *Angew. Chem.* **2013**, *125*, 4553–4557; c) J. Dong, F. Wang, J. You, *Org. Lett.* **2014**, *16*, 2884–2887; d) X. Li, Y.-H. Liu, W.-J. Gu, B. Li, F.-J. Chen, B.-F. Shi, *Org. Lett.* **2014**, *16*, 3904–3907; e) P. Subramanian, K. P. Kaliappan, *Eur. J. Org. Chem.* **2014**, 5986–5997; f) M. Shang, S.-Z. Sun, H.-L. Wang, B. N. Laforteza, H.-X. Dai, J.-Q. Yu, *Angew. Chem. Int. Ed.* **2014**, *53*, 10439–10442; *Angew. Chem.* **2014**, *126*, 10607–10610.

[38] G. J. Christian, A. Llobet, F. Maseras, *Inorg. Chem.* **2010**, *49*, 5977–5985.

[39] D. B. Collum, A. J. McNeil, A. Ramirez, *Angew. Chem. Int. Ed.* **2007**, *46*, 3002–3017; *Angew. Chem.* **2007**, *119*, 3060–3077.

[40] a) D. C. Powers, T. Ritter, *Nat. Chem.* **2009**, *1*, 302–309; b) N. R. Deprez, M. S. Sanford, *J. Am. Chem. Soc.* **2009**, *131*, 11234–11241; c) K. J. Stowers, M. S. Sanford, *Org. Lett.* **2009**, *11*, 4584–4587.

[41] M. Oyama, M. Goto, *Indian J. Chem. A* **2003**, *42A*, 733–738.

[42] L. Yang, Z. Lu, S. S. Stahl, *Chem. Commun.* **2009**, 6460–6462.

[43] The structure was confirmed by comparison with independently prepared **1**-Cl, shown in Scheme S10.

[44] The resting state of a catalyst sometimes is found outside of the catalytic cycle and might be the only catalytic species observed; see: a) F. Paul, J. Patt, J. F. Hartwig, *J. Am. Chem. Soc.* **1994**, *116*, 5969–5970; b) G. P. F. van Strijdonck, M. D. K. Boele, P. C. J. Kamer, J. G. de Vries, P. W. N. M. van Leeuwen, *Eur. J. Inorg. Chem.* **1999**, 1073–1076; c) T. Rosner, J. L. Bars, A. Pfaltz, D. G. Blackmond, *J. Am. Chem. Soc.* **2001**, *123*, 1848–1855; d) G.-J. t. Brink, I. W. C. E. Arends, R. A. Sheldon, *Adv. Synth. Catal.* **2002**, *344*, 355–369; e) E. Alvaro, J. F. Hartwig, *J. Am. Chem. Soc.* **2009**, *131*, 7858–7868; f) Z. Shen, P. K. Dornan, H. A. Khan, T. K. Woo, V. M. Dong, *J. Am. Chem. Soc.* **2009**, *131*, 1077–1091.

[45] A growing number of Cu^{III} species resulting from disproportionation of two copper(II) centers have been observed and characterized (e.g., see ref.[3c]) They have been shown as competent intermediates to undergo reductive elimination. However, the majority of the reported copper(III) species are stabilized by macrocyclic arene ligands. Without the stabilizing ligands, the copper(III) intermediate may have been skipped (i.e., no longer a local minimum) on the reaction potential energy surface. In its place, two copper(II) centers may undergo a collective two-electron transfer "reductive elimination" to afford the oxidized product and two copper(I) centers. The difference between the "concerted" [i.e., no copper(III)] and "stepwise" [i.e., copper(III) is an intermediate] is energetically subtle but consequential in guiding catalyst development in copper-mediated reactions. This argument clearly needs to be tested further in future studies.

[46] L. Ling, J. Chen, J. Song, Y. Zhang, X. Li, L. Song, F. Shi, Y. Li, C. Wu, *Org. Biomol. Chem.* **2013**, *11*, 3894–3902.

[47] The M–M distance is ca. 2.6 Å for acetate-supported dicopper(II) and ca. 2.8 Å for acetate-supported dipalladium(II).

[48] D. C. Powers, D. Benitez, E. Tkatchouk, W. A. Goddard, T. Ritter, *J. Am. Chem. Soc.* **2010**, *132*, 14092–14103.

[49] a) K. D. Karlin, R. W. Cruse, Y. Gultneh, *J. Chem. Soc., Chem. Commun.* **1987**, 599–600; b) P. Ghosh, Z. Tyeklar, K. D. Karlin, R. R. Jacobson, J. Zubieta, *J. Am. Chem. Soc.* **1987**, *109*, 6889–6891.

[50] **D** and **E** might be the sources of the oxygenation reaction to afford the hydroxylated imine. However, at this point we do not have an experimentally tested model to describe this side reaction.

[51] H. Sigel, C. Flierl, R. Griesser, *J. Am. Chem. Soc.* **1969**, *91*, 1061–1064.

[52] I. Kaljurand, A. Kütt, L. Sooväli, T. Rodima, V. Mäemets, I. Leito, I. A. Koppel, *J. Org. Chem.* **2005**, *70*, 1019–1028.

[53] A. Kütt, I. Leito, I. Kaljurand, L. Sooväli, V. M. Vlasov, L. M. Yagupolskii, I. A. Koppel, *J. Org. Chem.* **2006**, *71*, 2829–2838.

[54] M. C. Paderes, L. Belding, B. Fanovic, T. Dudding, J. B. Keister, S. R. Chemler, *Chem. Eur. J.* **2012**, *18*, 1711–1726.

[55] Similar to the current work, the resting state was structurally characterized, whereas the structure of the in-cycle active catalyst engaging in turnover was inferred.

[56] A. E. King, B. L. Ryland, T. C. Brunold, S. S. Stahl, *Organometallics* **2012**, *31*, 7948–7957.

[57] A similar situation was found in palladium catalysis, for which both half order and second order in palladium were reported; see ref.[40,44b,44c,58]

[58] G.-J. t. Brink, I. W. C. E. Arends, G. Papadogianakis, R. A. Sheldon, *Appl. Catal. A* **2000**, *194–195*, 435–442.

[59] M. He, G. Chen, X. Huang, R. Xu, Z. Zeng, J. Yang, *Polym. Chem.* **2014**, *5*, 2951–2960.

[60] a) M. Weiss, M. Appel, *J. Am. Chem. Soc.* **1948**, *70*, 3666–3667; b) M. L. Lewbart, V. R. Mattox, *J. Org. Chem.* **1963**, *28*, 2001–2006.

[61] S. Kambourakis, J. W. Frost, *J. Org. Chem.* **2000**, *65*, 6904–6909.

[62] We did not model the postulated mechanism computationally, because we do not have the expertise to do so or to interpret such data with confidence at this point.

[63] L. Que Jr., W. B. Tolman, *Nature* **2008**, *455*, 333–340.

[64] a) V. Diez, J. V. Cuevas, G. García-Herbosa, G. Aullón, J. P. H. Charmant, A. Carbayo, A. Muñoz, *Inorg. Chem.* **2007**, *46*, 568–577; b) C.-H. Chien, S. Fujita, S. Yamoto, T. Hara, T. Yamagata, M. Watanabe, K. Mashima, *Dalton Trans.* **2008**, 916–923.

[65] F. M. Garibotto, M. A. Sortino, V. V. Kouznetsov, R. D. Enriz, S. A. Zacchino, *ARKIVOC (Gainesville, FL, U.S.)* **2011**, 149–161.

[66] H. A. Michaels, C. S. Murphy, R. J. Clark, M. W. Davidson, L. Zhu, *Inorg. Chem.* **2010**, *49*, 4278–4287.

[67] P. Bandyopadhyay, S. Jha, S. K. I. Ali, *J. Agric. Food Chem.* **2009**, *57*, 9780–9786.

[68] V. V. Kouznetsov, L. Y. V. Méndez, M. Sortino, Y. Vásquez, M. P. Gupta, M. Freile, R. D. Enriz, S. A. Zacchino, *Bioorg. Med. Chem.* **2008**, *16*, 794–809.

[69] Z. Zheng, G. Zhao, R. Fablet, M. Bouyahyi, C. M. Thomas, T. Roisnel, O. C. Jr., J.-F. Carpentier, *New J. Chem.* **2008**, *32*, 2279–2291.

[70] A. Begouin, M.-J. R. P. Queiroz, *Eur. J. Org. Chem.* **2009**, 2820–2827.

Received: May 9, 2016
Published Online: July 19, 2016

 © 2016 Wiley-VCH Verlag GmbH & Co. KGaA, Weinheim